About Omics Group

OMICS Group International through its Open Access Initiative is committed to make genuine and reliable contributions to the scientific community. OMICS Group hosts over 400 leading-edge peer reviewed Open Access Journals and organize over 300 International Conferences annually all over the world. OMICS Publishing Group journals have over 3 million readers and the fame and success of the same can be attributed to the strong editorial board which contains over 30000 eminent personalities that ensure a rapid, quality and quick review process.

About Omics Group conferences

- OMICS Group signed an agreement with more than 1000 International Societies to make healthcare information Open Access. OMICS Group Conferences make the perfect platform for global networking as it brings together renowned speakers and scientists across the globe to a most exciting and memorable scientific event filled with much enlightening interactive sessions, world class exhibitions and poster presentations
- Omics group has organised 500 conferences, workshops and national symposium across the major cities including SanFrancisco,Omaha,Orlado,Rayleigh,SantaClara,Chicago,Philadelphia,Unitedkingdom,Baltimore,SanAntanio,Dubai,Hyderabad,Bangaluru and Mumbai.

Charge Transfer in Nanostructures for Solar Energy and Biochemical Detector Applications

Branislav Vlahovic

Physics Department, North Carolina Central University, E-mail: vlahovic@nccu.edu

Lasers Optics & Photonics
September 10, 2014
Philadelphia

Confinement in nanostrucutres

Multijunction

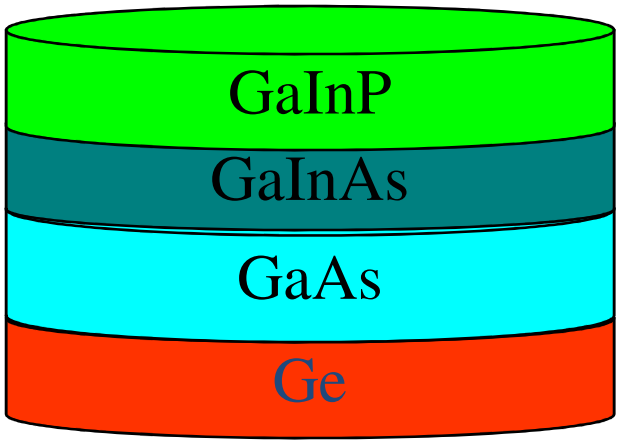

Quantum Dot

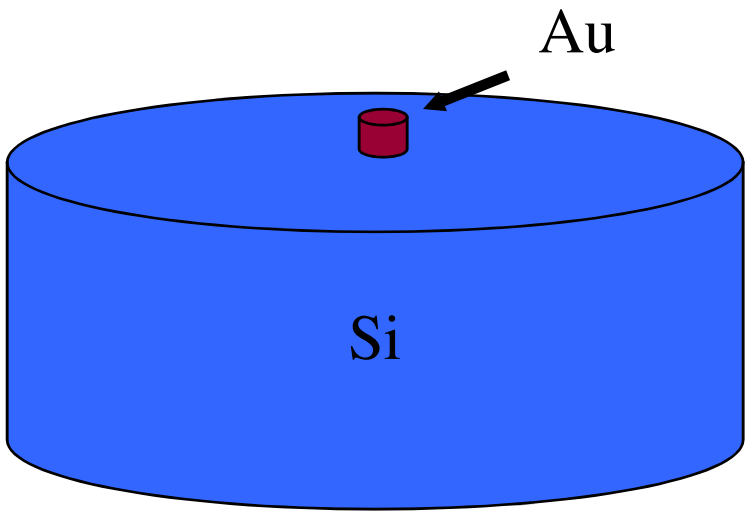

Electron Energy Levels in quantum dots

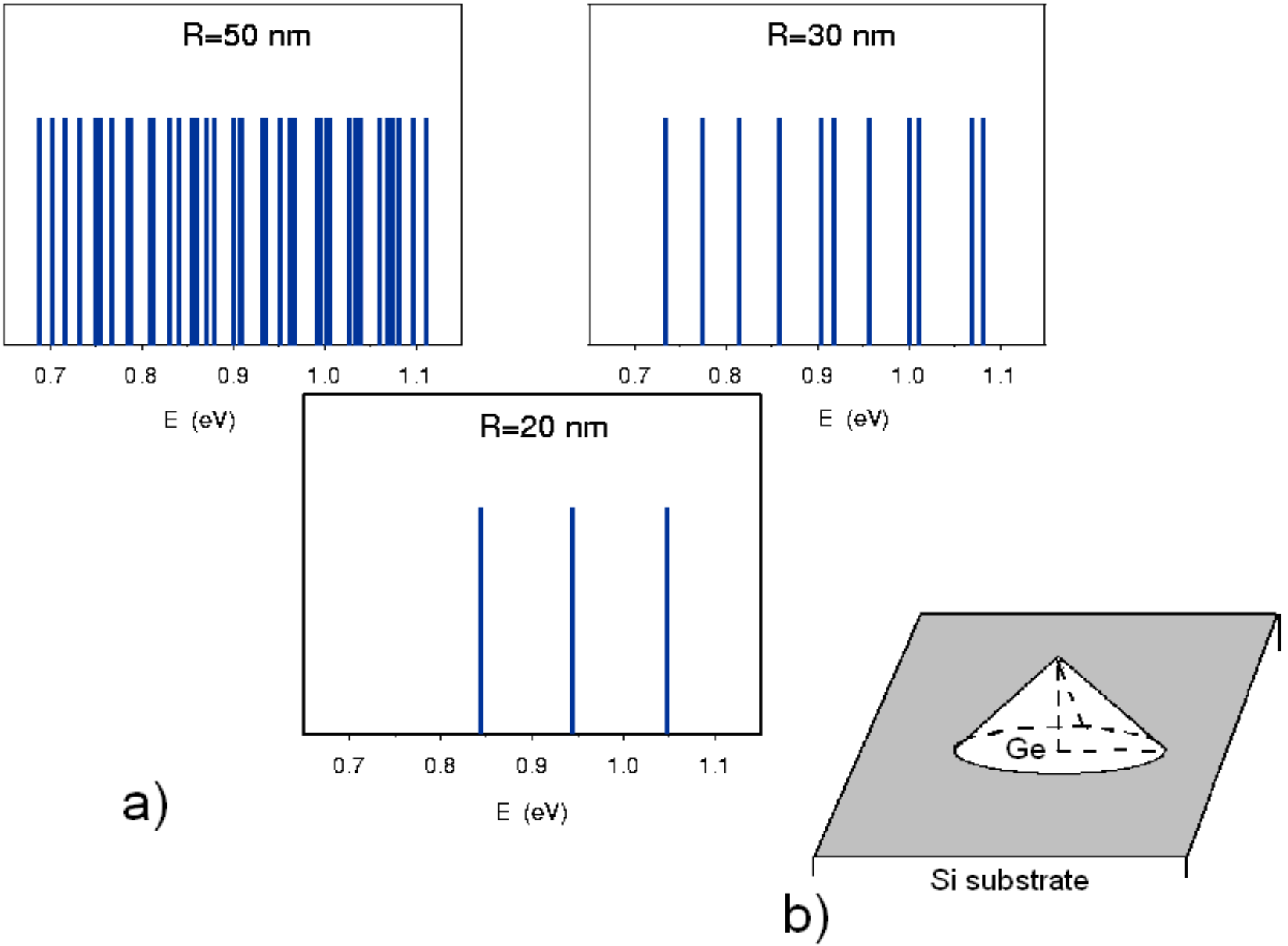

Square of electron wave functions in QD

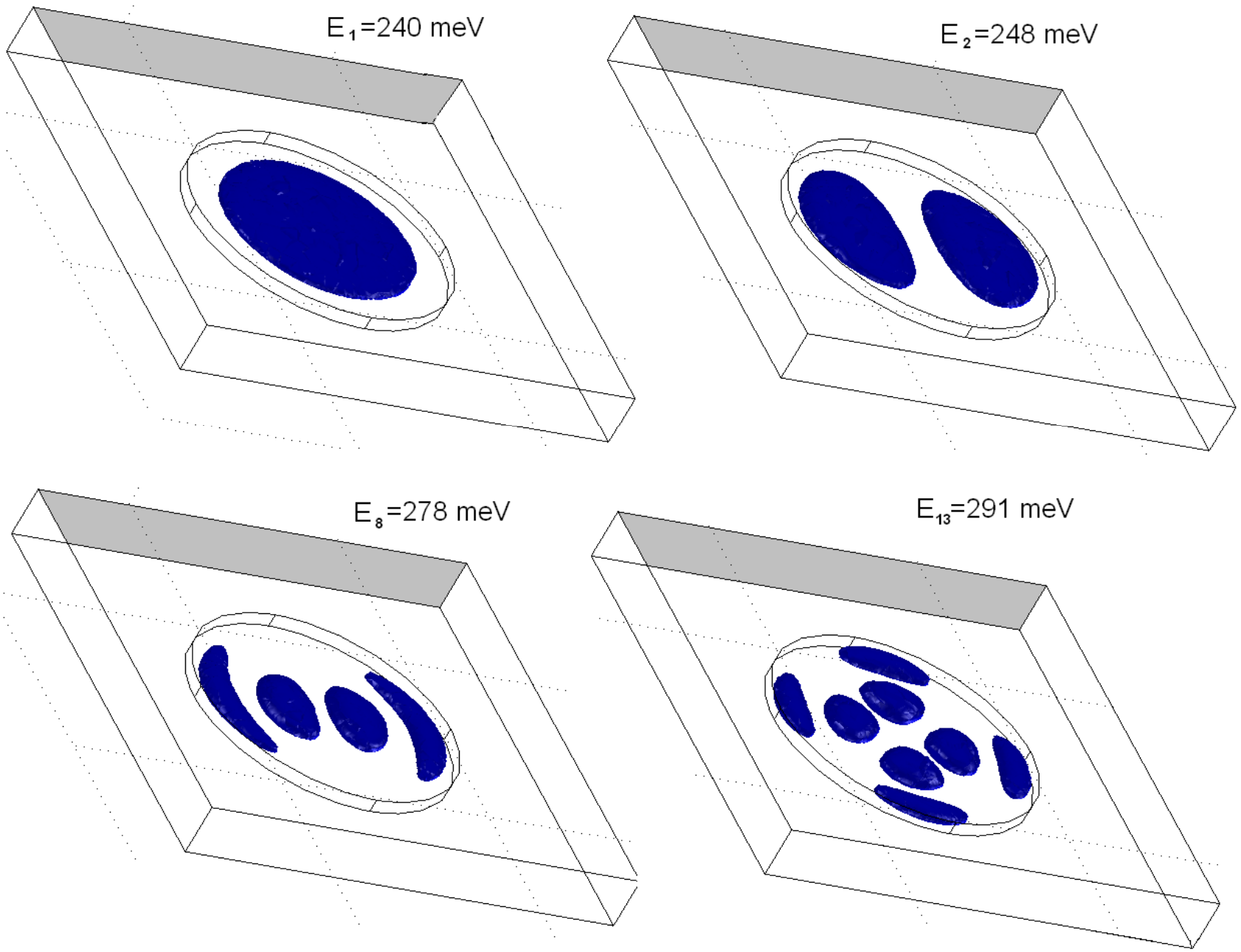

Quantum Dot Solar Cells

- **Tunable bandgaps**
  - **Optimize overlap with solar spectrum**
  - **Use single semiconductor for multi-junction cells**
- **Slowed carrier cooling – "hot" carrier extraction**
- **Impact ionization – multiple carriers generated from single photon**
- **High resistance to photobleaching, thermal decomposition**

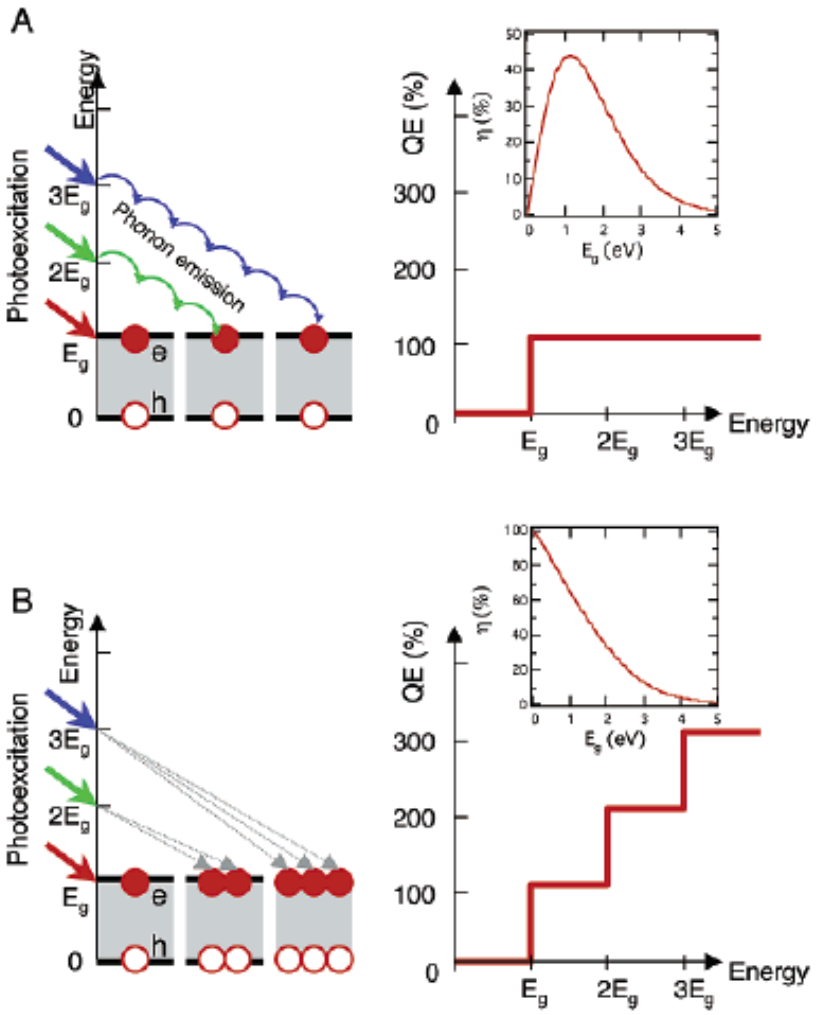

Schaller, et al *Nano Lett.* **6**, 424 (2006).

Nanowire Solar Cells

- **High crystalline quality**
  - **Excellent charge transport along wire axis**
  - **Strain relief: No substrate lattice matching substrate required (e.g. GaAs or InP on Si)**
- **Increased light absorption**
  - **Resonance enhancement**
  - **Light trapping**
  - **Reduced material usage**
- **Single nanowire solar cells**
  - **Radial / axial heterostructures**
  - **Improved carrier separation**
  - **Reduced recombination (short diffusion lengths)**
- **Sensitized (QD, dye, perovskite) structures also possible**

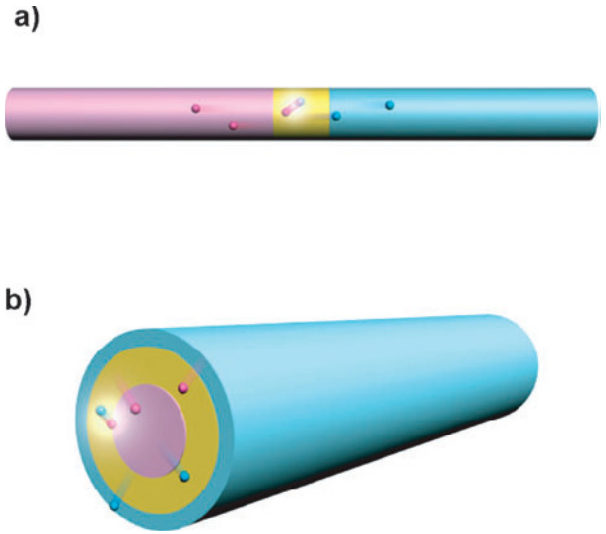

Tian, et al Chem. Soc. Rev. 38, 16 (2009)

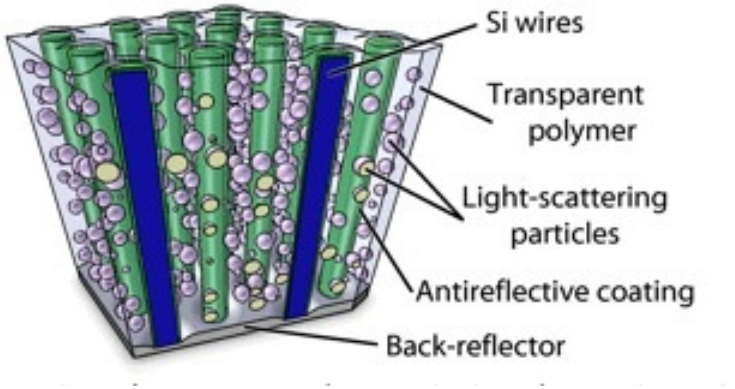

H Atwater, Caltech

New Type of Biochemical detector – New Principle of Operation

- **Highly selective**
- **Highly sensitive**
- **Detect analyte**
- **Distinguish between various analytes**
- **Determine analyte quantity**
- **Isolate, extract and manipulate analyte**

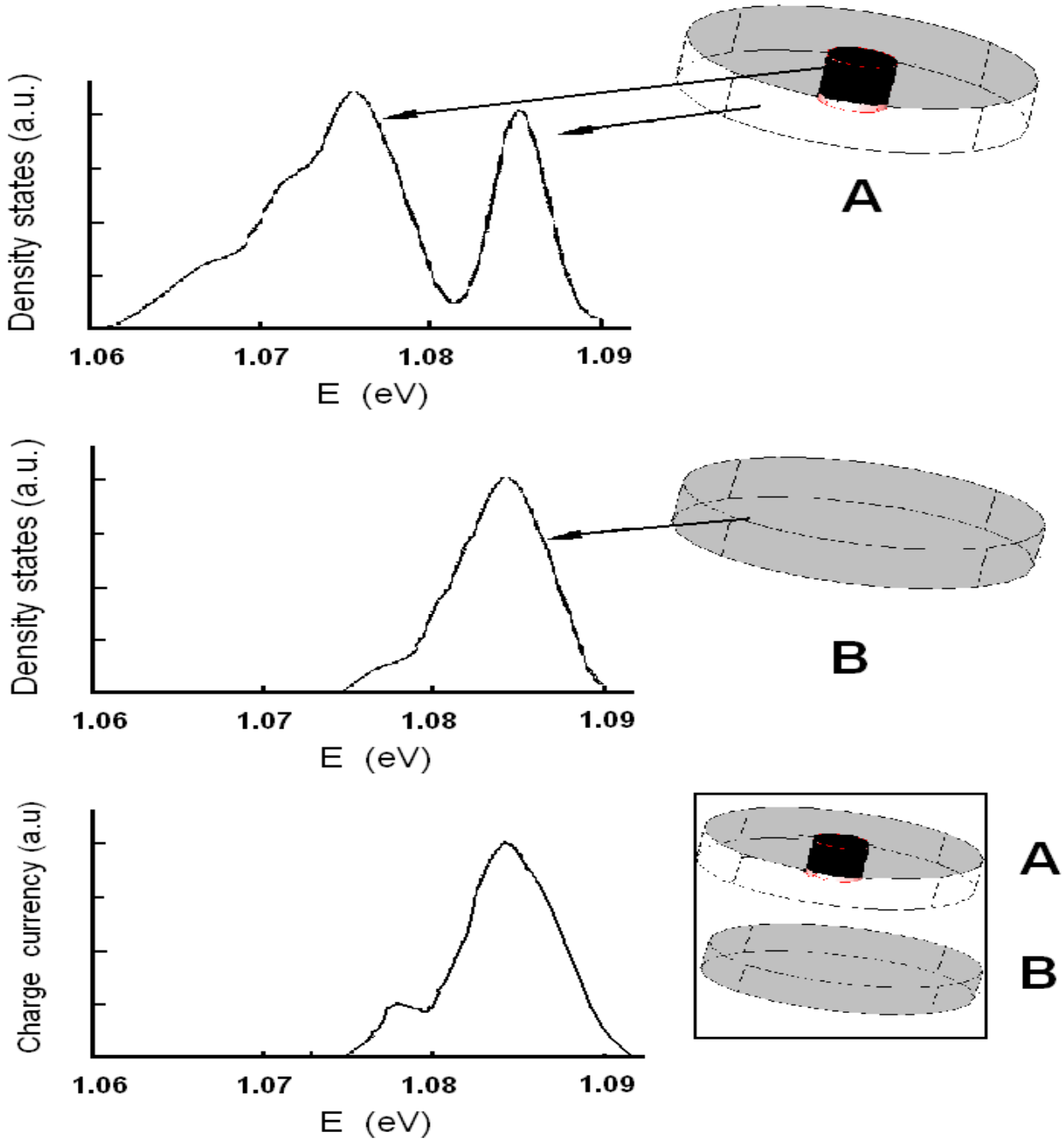
Density states (a.u.)
1.06
1.07
1.08
1.09
E (eV)
A
Density states (a.u.)
1.06
1.07
1.08
1.09
E (eV)
B
Charge currency (a.u)
1.06
1.07
1.08
1.09
E (eV)
A
B

Fig. 10

SCHEMATIC
of how the QD biosensor works

Case 1

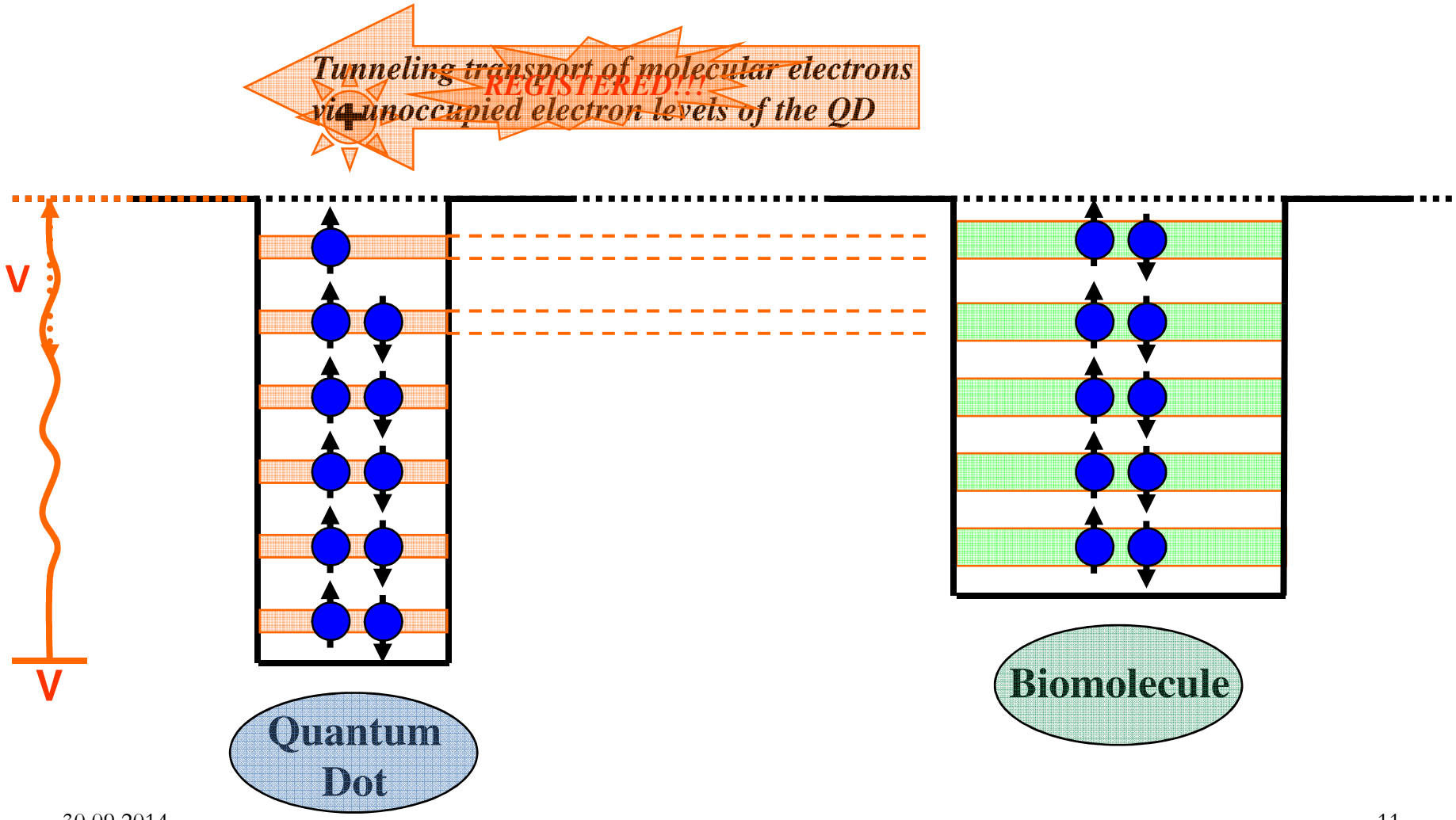

SCHEMATIC
of how the QD biosensor works

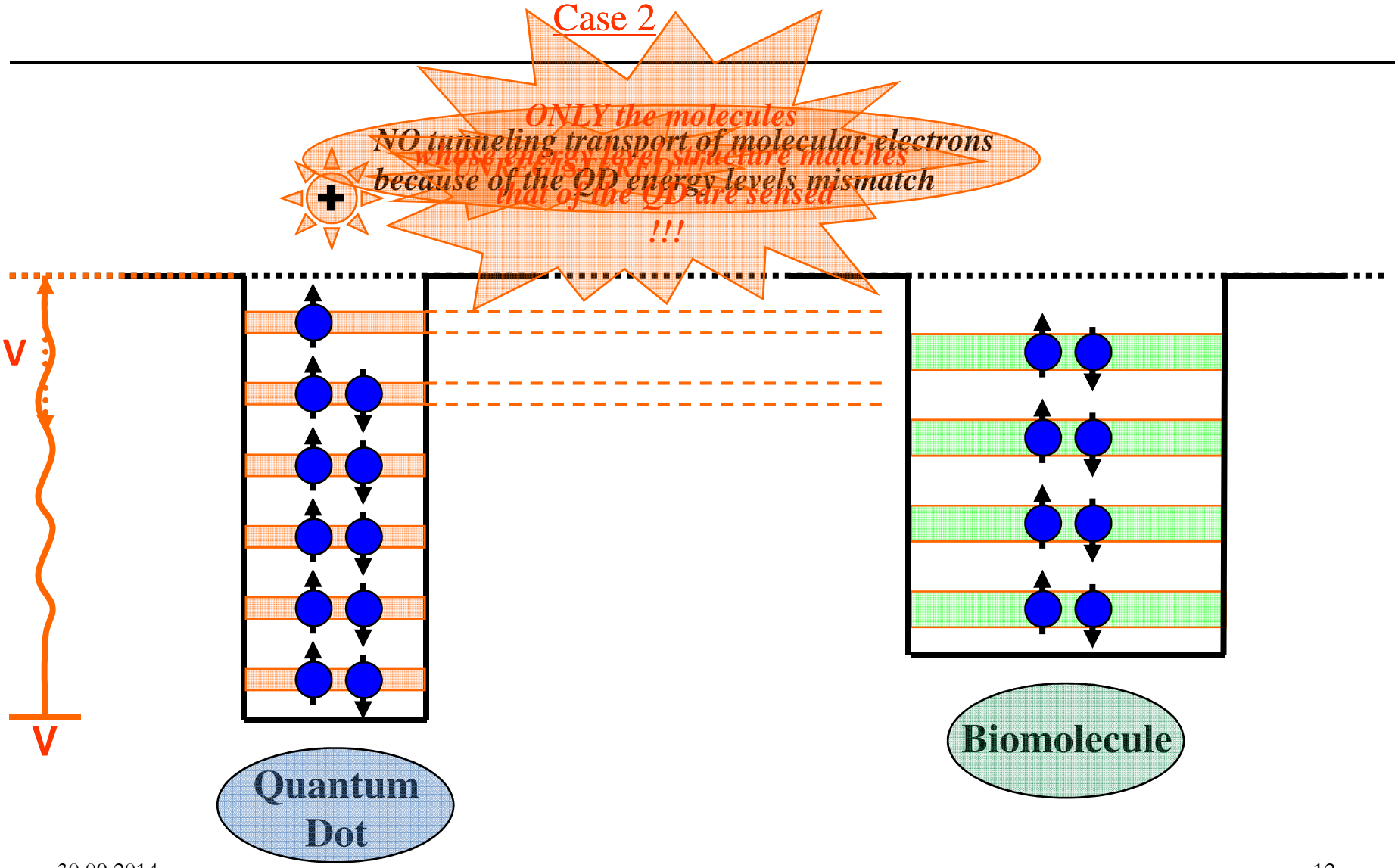

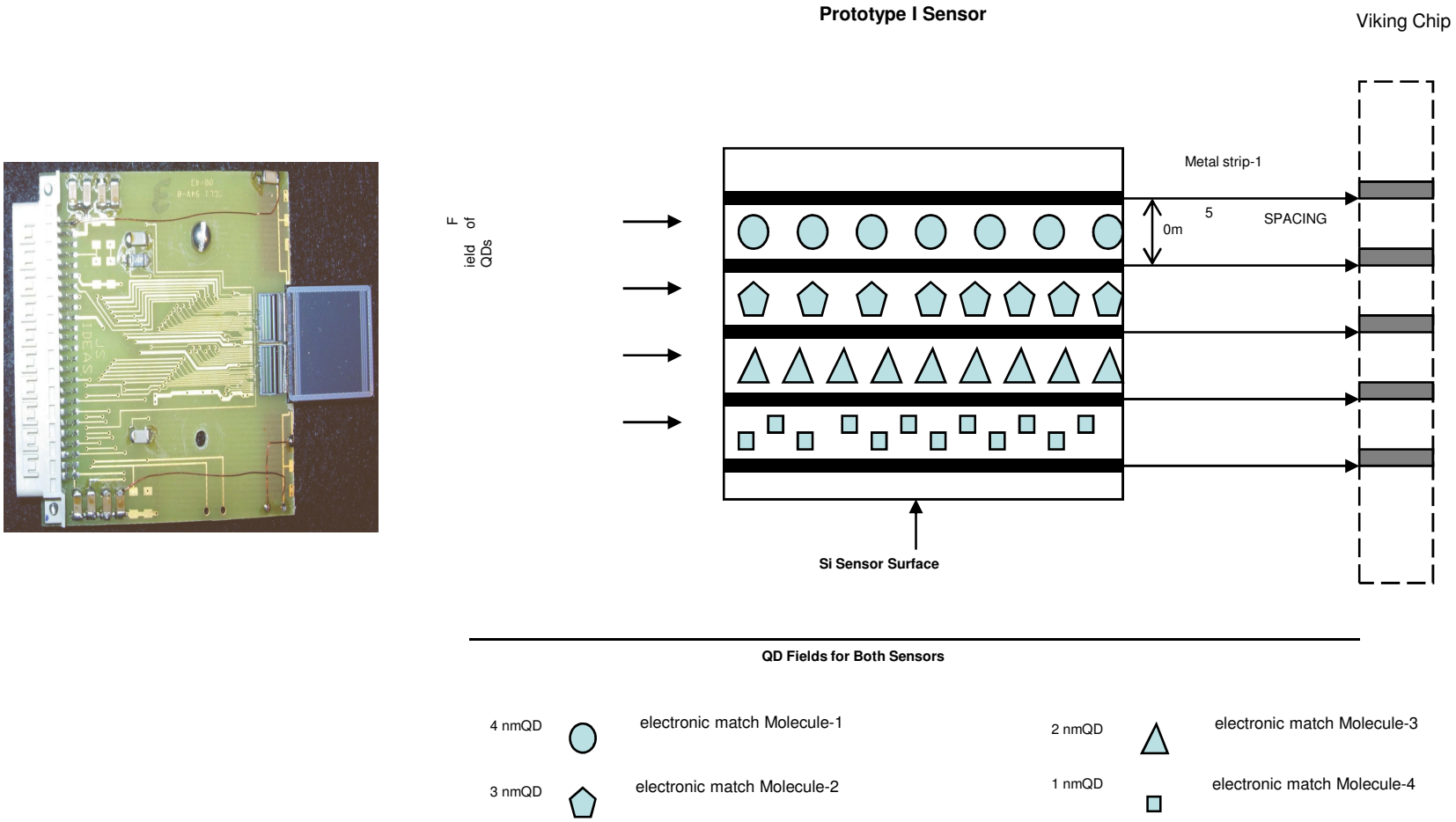

Figure 1. (r) Schematic of QD biochemical sensor, (l) microstrip detector.

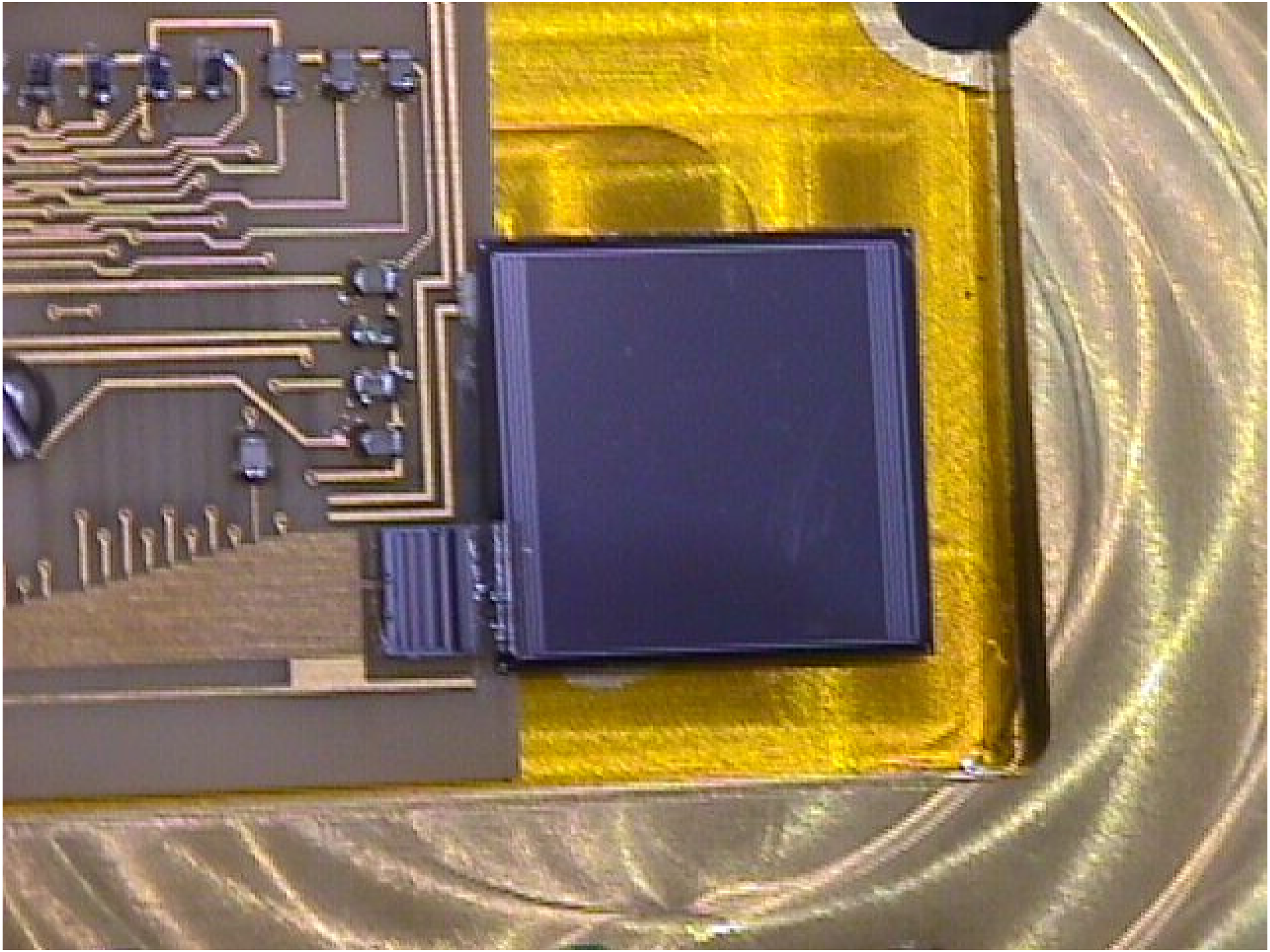

Cursor Marker Spectrum Zoom Center Line Offset Clear

Section Analysis

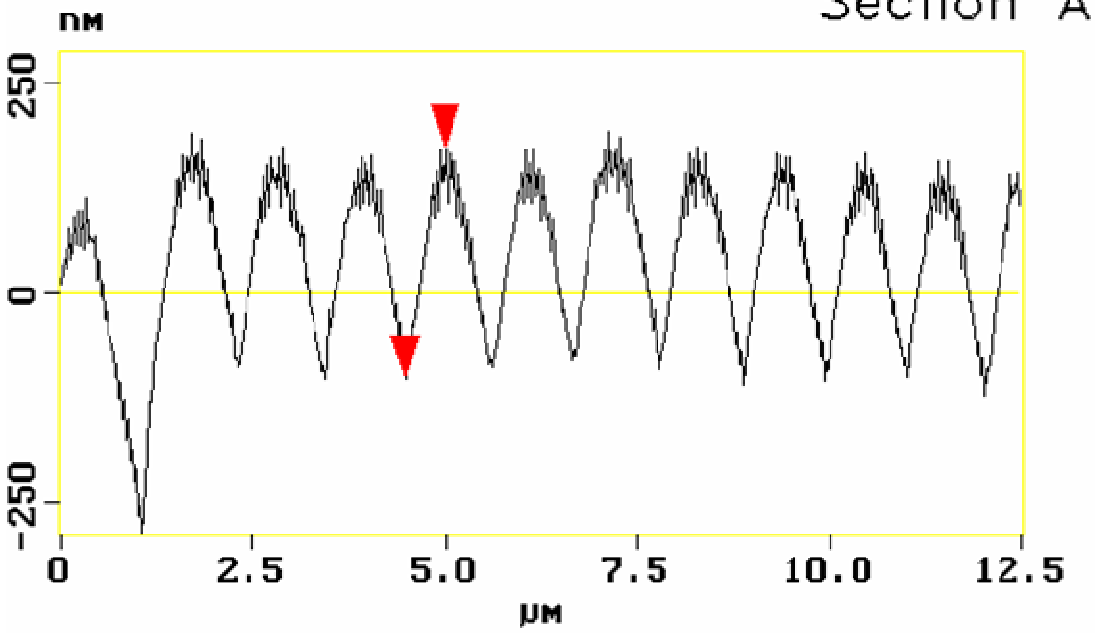

L	512.70 nm
RMS	82.317 nm
lc	DC
Ra(lc)	12.184 nm
Rmax	68.434 nm
Rz	47.929 nm
Rz Cnt	8

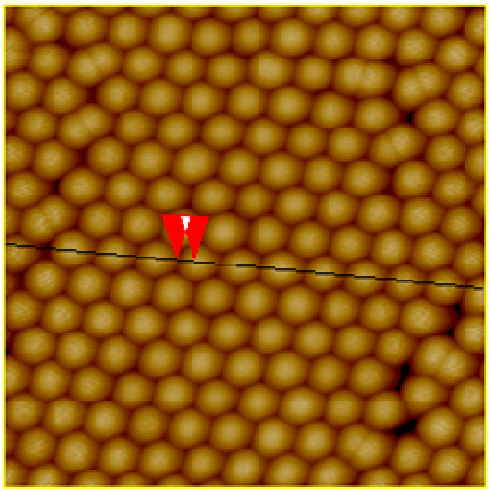

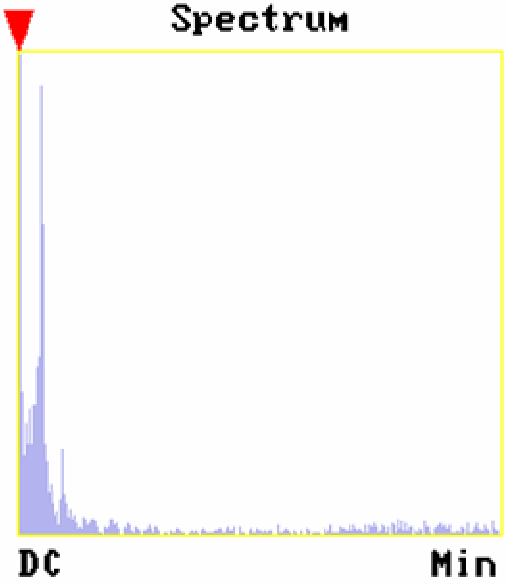

Surface distance	773.75 nm
Horiz distance(L)	512.70 nm
Vert distance	274.21 nm
Angle	28.140 deg
Surface distance	
Horiz distance	
Vert distance	
Angle	
Surface distance	
Horiz distance	
Vert distance	
Angle	
Spectral period	DC
Spectral freq	0 Hz
Spectral RMS amp	0.058 nm

as040201.005

Cursor: fixed Zoom: 2:1 Cen line: Off Offset: Off

PLD Nanostructure production

- Quantum dots
  - 1 – 20 nm single element (Si, Ge), binary (InP, GaAs, InAs)
  - Size control via laser fluence, backing gas pressure
  - Desired stoichiometry at optimized parameters (RBS, SEM – EDX)
- Nanowires
  - 10 – 100 nm II-VI (CdS), IV (Si, Ge), II-V (In_2Se_3) nanowires
  - Good stoichiometry (SEM-EDX), crystalline structure (SEM – EBSD)

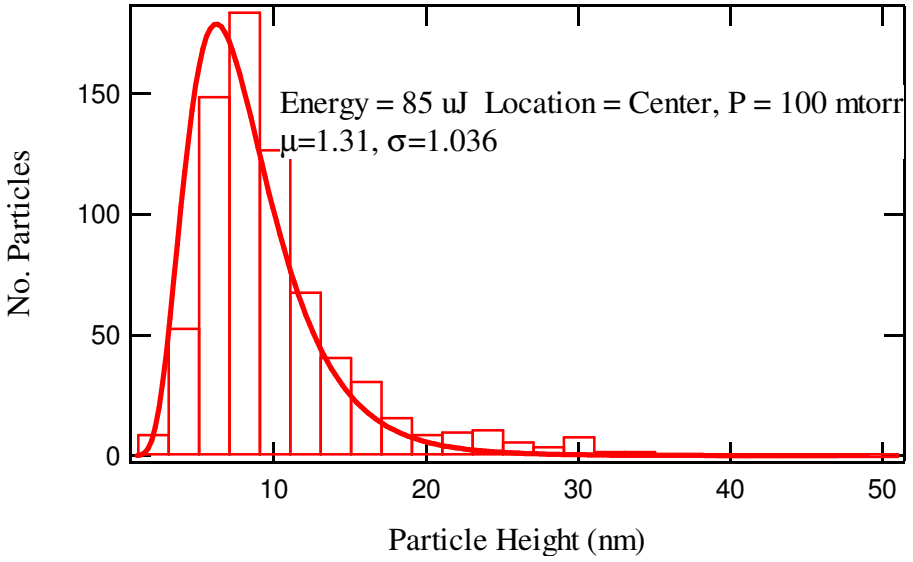

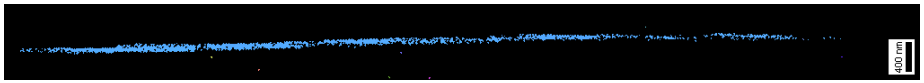

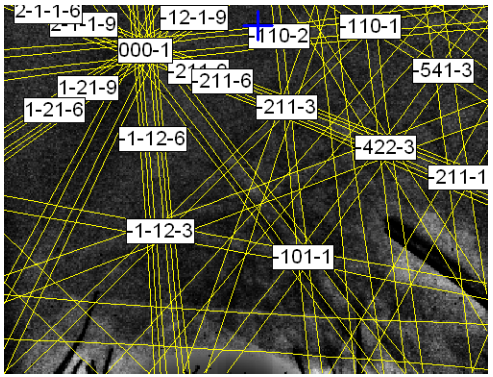

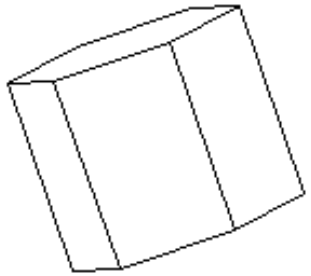

Size Dependence on Sampling Site

Edge (~ 6 mm from center)

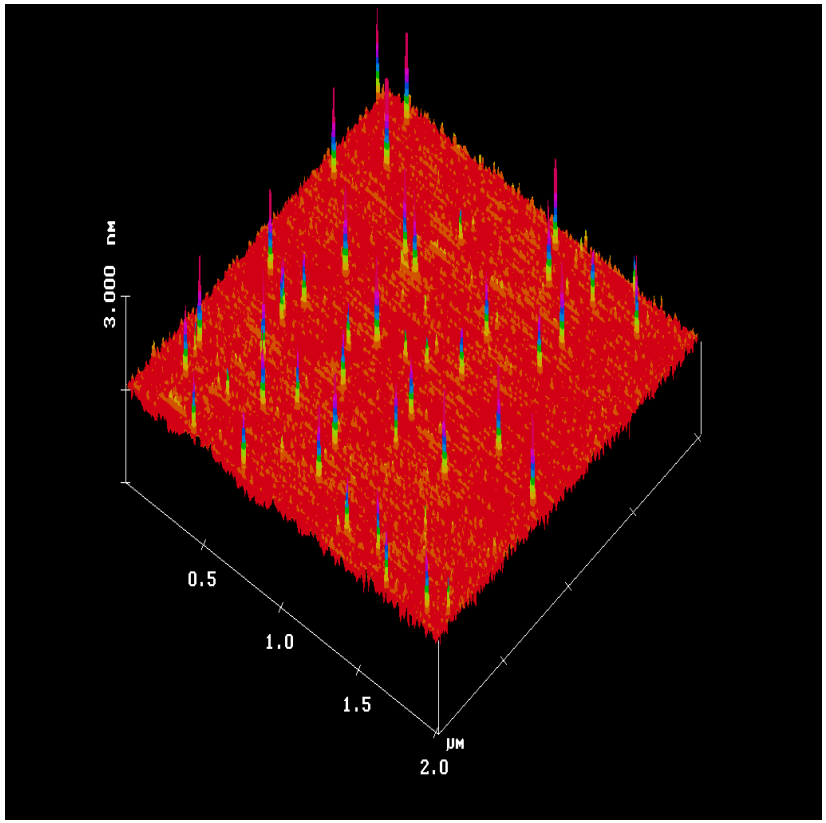

- Full scale = 1.5 nm
- Average size = 1.4 nm

Center

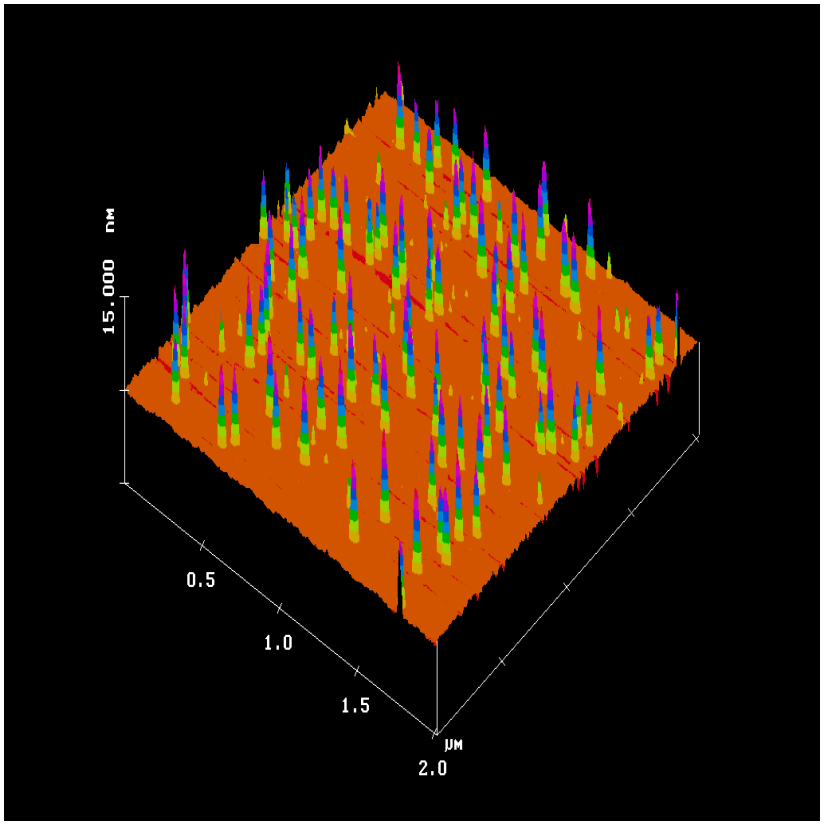

- Full scale= 7.5 nm
- Average size = 5.3 nm

QD Size Control: Laser Fluence

1.0 J/cm^2

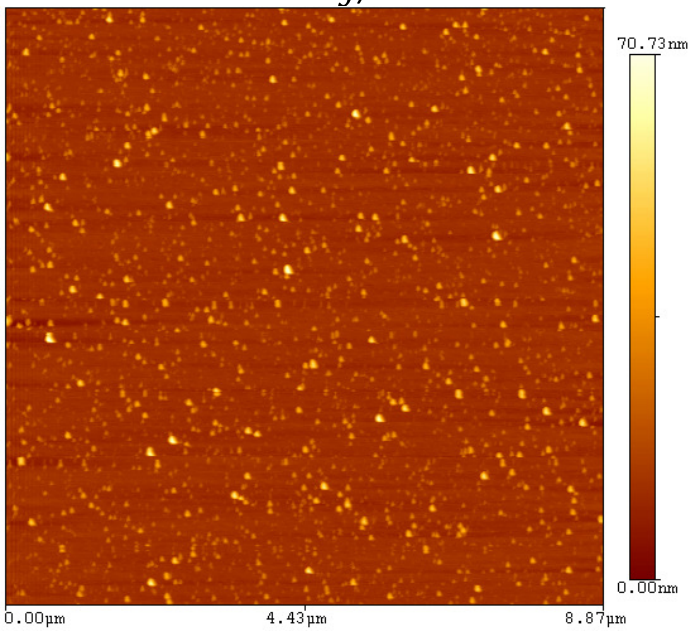

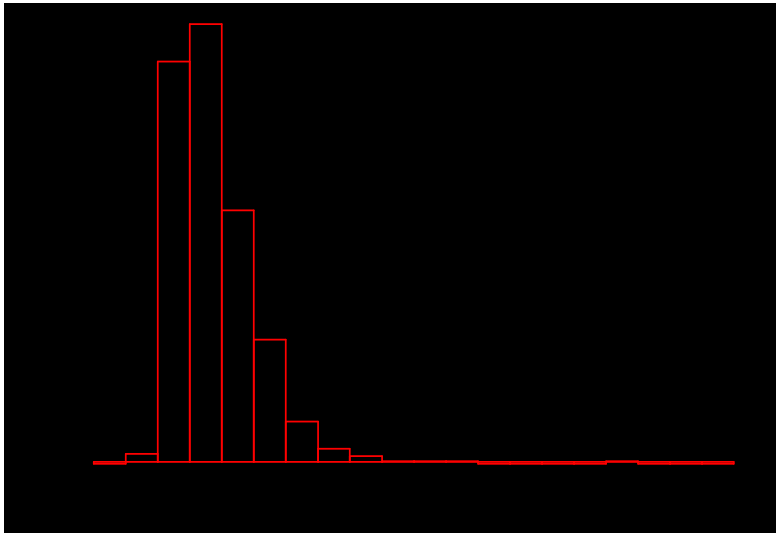

0.15 J/cm^2

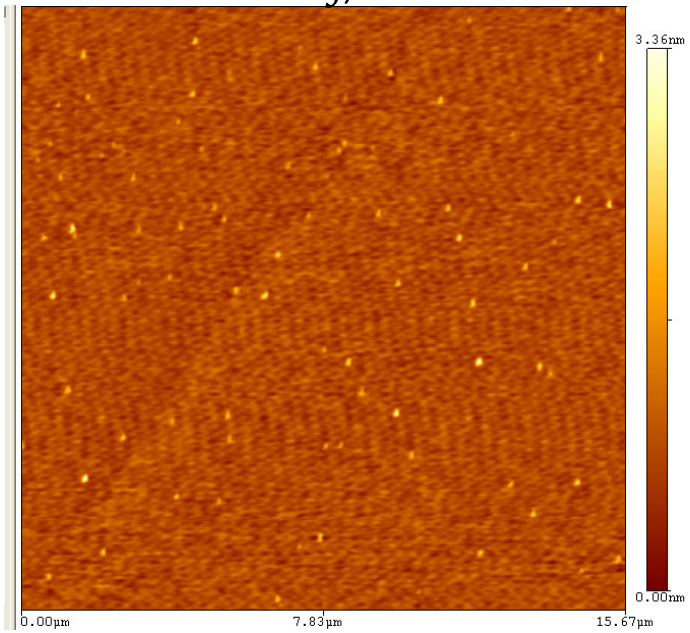

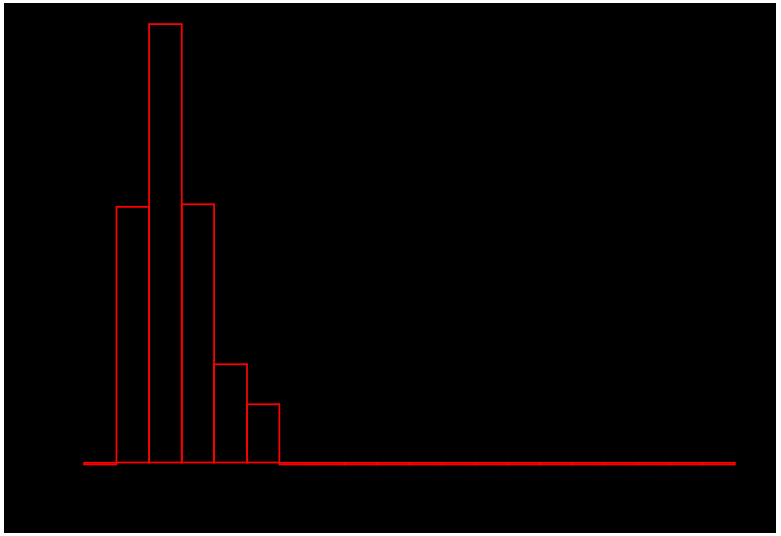

Effective model for InAs quantum dot in GaAs substrate

Geometry model

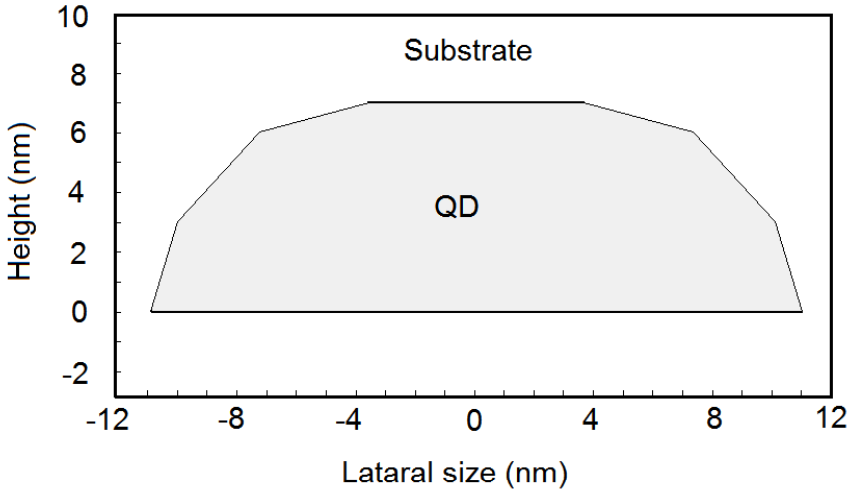

Cross sections of QD

Formalism :

- *kp-perturbation theory in a single subband approach*

[Luttinger J. M. and Kohn W. Phys. Rev. 97, 869 (1955)]

- *Energy dependent quasi-particle effective mass approximation (non-parabolic approach)*

[Kane E. J. Phys. Chem. Solids, 1, 249 (1957)]

Formalism

Schrödinger equation with energy dependence of the effective mass

$$\left(H_{kp}+V_c(\mathbf{r})+V_s(\mathbf{r})\right)\Psi(\mathbf{r})=E\Psi(\mathbf{r}),$$

$$H_{kp}=-\nabla\frac{\hbar^2}{2m^*(E,\mathbf{r})}\nabla$$

- the one band kp Hamiltonian operator

$$m^*(E,\mathbf{r})=\begin{cases} m^*_{QD}(E), & r\in QD,\\ m^*_{Substrate}(E), & r\in Substrate,\end{cases}$$

- the carrier effective mass

$$(n,\frac{1}{m^*(E,\mathbf{r})}\nabla\Psi)=0$$

- is continuous on the surface of QD/Substrate interface

Iterative method of solution:

$$H(m_i^{*,n-1})\Phi^n=E^n\Phi^n$$

$$m_i^{*,n}=f_i\left(E^n\right)$$

Energy dependence of effective mass

Kane's formula:

$$\frac{m_0}{m^*} = \frac{2m_0 P^2}{3\hbar^2}\left(\frac{2}{E_g + E} + \frac{1}{E_g + \Delta + E}\right).$$

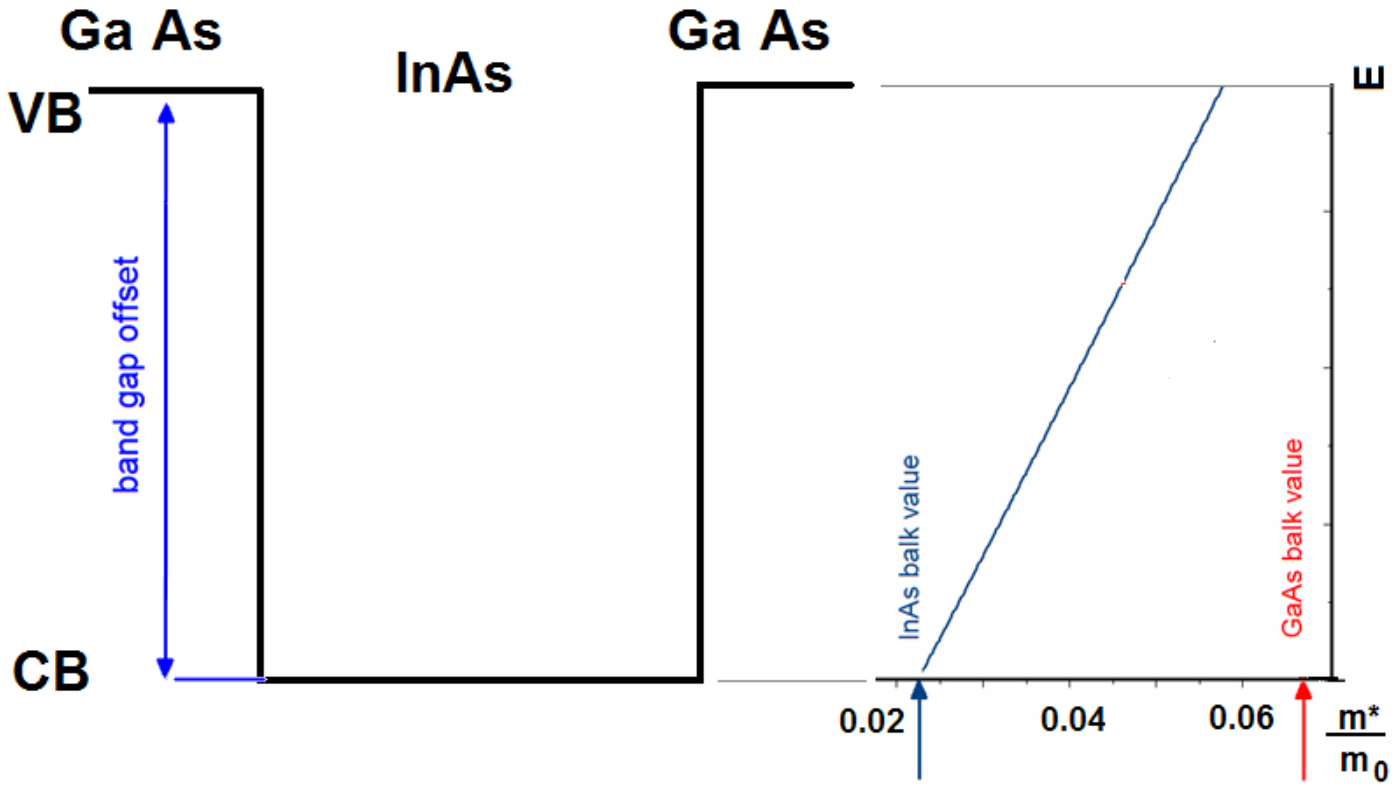

Effective potential for strained quantum structures

the band gap potential

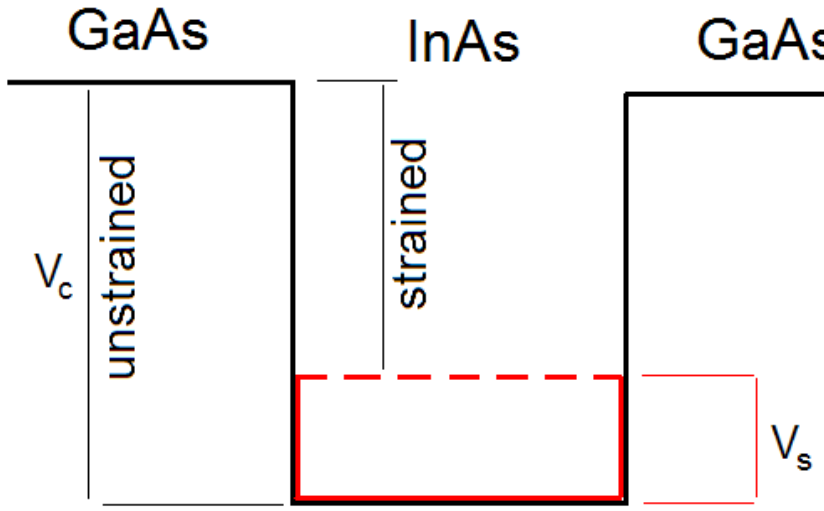

the effective potential

$$V_c(\mathbf{r}) = \begin{cases} 0, & \in QR, \\ E_c, r \notin QR, \text{ where} \end{cases}$$

E_c

CB band gap alignment for QD/Substrate materials

Effective model and band gap structure

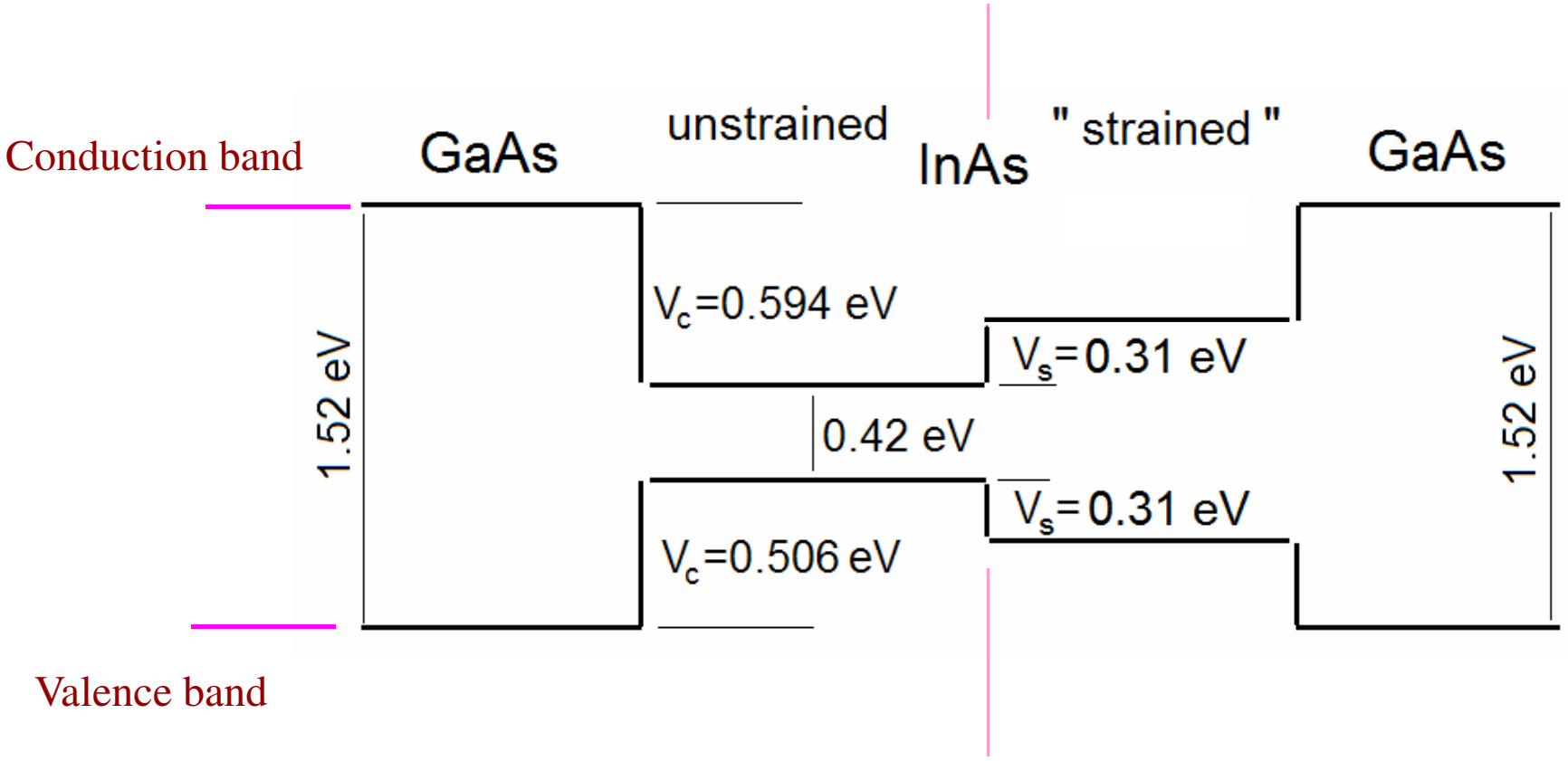

Capacitance spectroscopy modeling

Electron levels of InAs/GaAs quantum dots: perturbation theory calculations

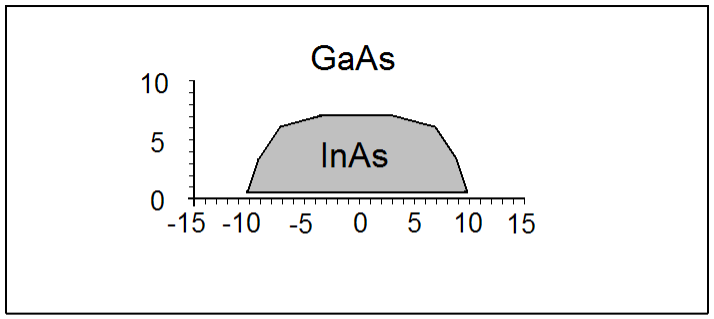

I. Filikhin, V. M. Suslov and B. Vlahovic, Phys. Rev. B 73, 205332 (2006).

I.Filikhin, E. Deyneka and B. Vlahovic, Sol. Stat. Comm. 140, 483 (2006)

M. Grundmann, et al., Phys. Rev. B 52, 11969,(1995);
O. Stier, et al. Phys. Rev. B 59, 5688,(1999).
C. Pryor, Phys. Rev. B 57, 7190, 1998.

for "*ab initio*" calculation:

$V_s = 0.21$ eV

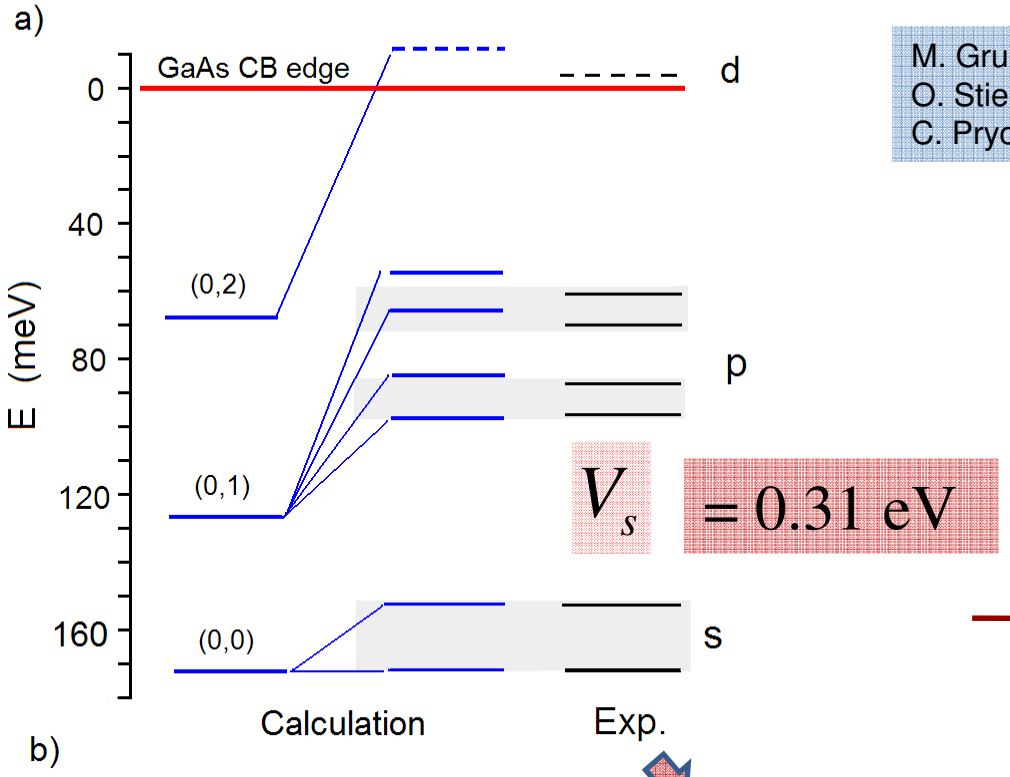

$V_s = 0.31$ eV

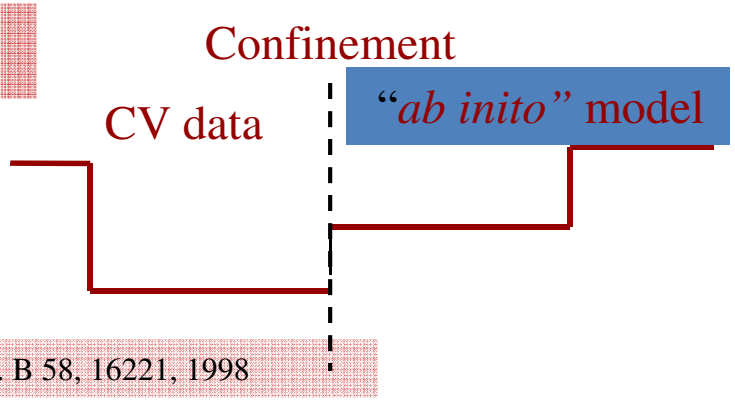

R. J. Warburton, et al., Phys. Rev. B 58, 16221, 1998

"Ab initio" models and CV data

A. Lorke, et al., Phys. Rev. Lett. 84, 2223 (2000)

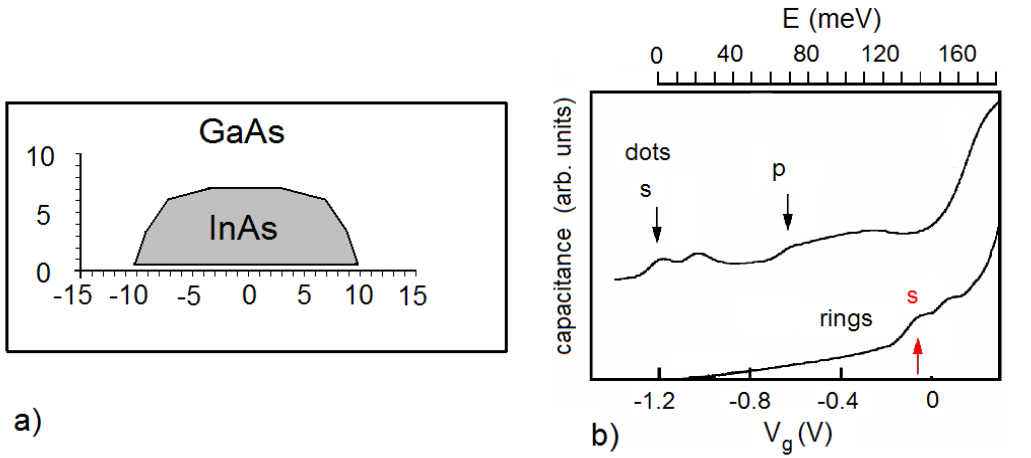

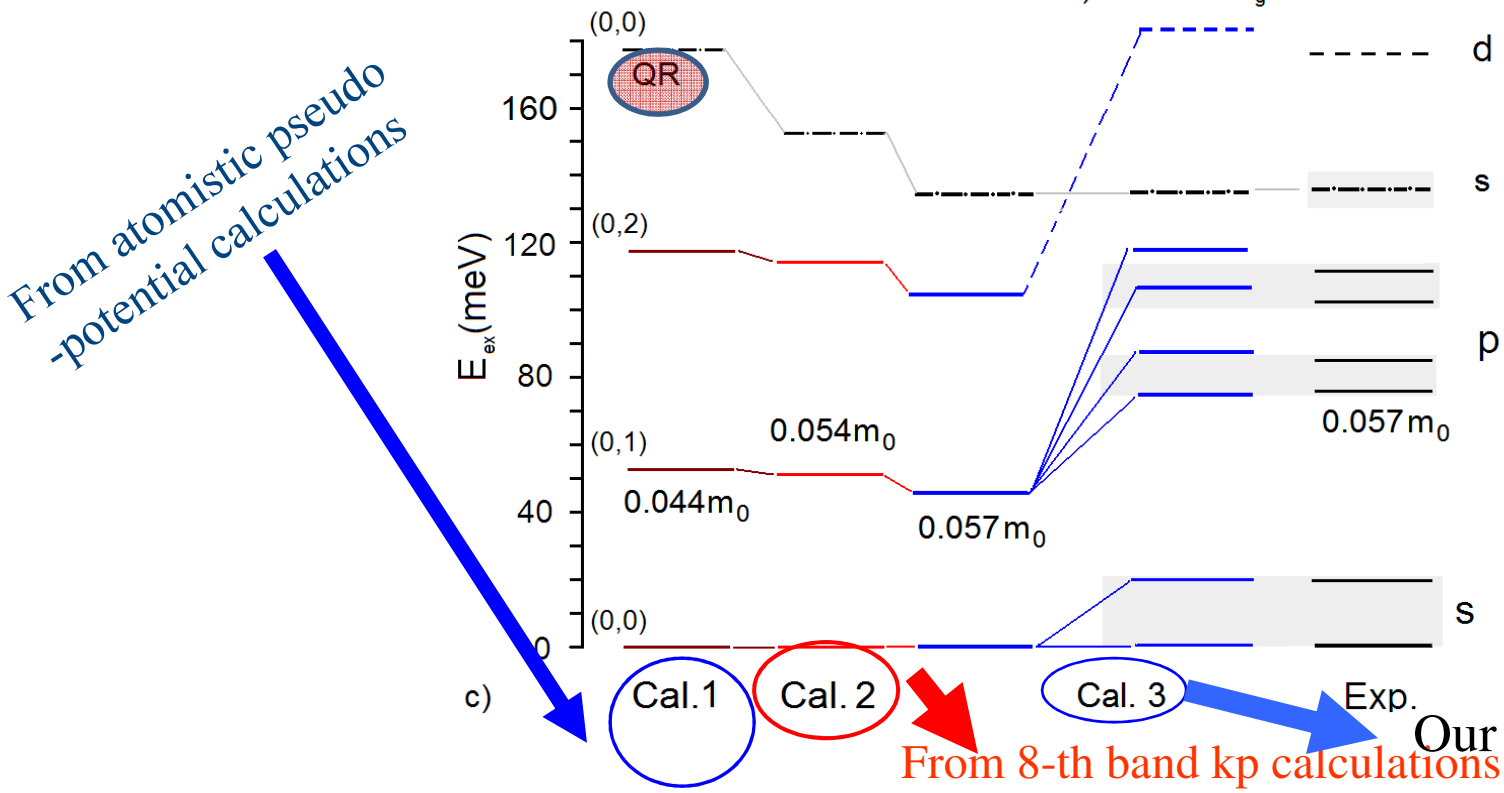

Material mixing of QD/substrate

Strain and Interdiffusion in InAsGaAs Quantum Dots:

I. Kegel, T. H. Metzger, A. Lorke, J. Peisl, J. Stangl, G. Bauer, J. M. García, P. M. Petroff, *Phys. Rev. Lett.* **85**, 1694, 2000.

InAs/GaAs QD: **Model 1** - from

A. Schliwa, M. Winkelnkemper and D. Bimberg, Phys. Rev. 76, 205324 (2007)

$V^e{}_s = 0.21$ eV

$V^h{}_s = 0.28$ eV

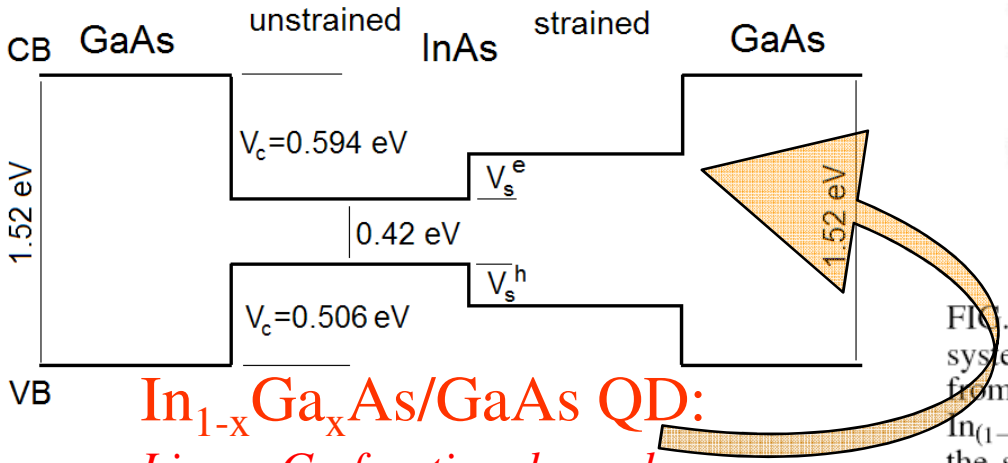

$In_{1-x}Ga_xAs/GaAs$ QD:

Linear Ga fraction dependence

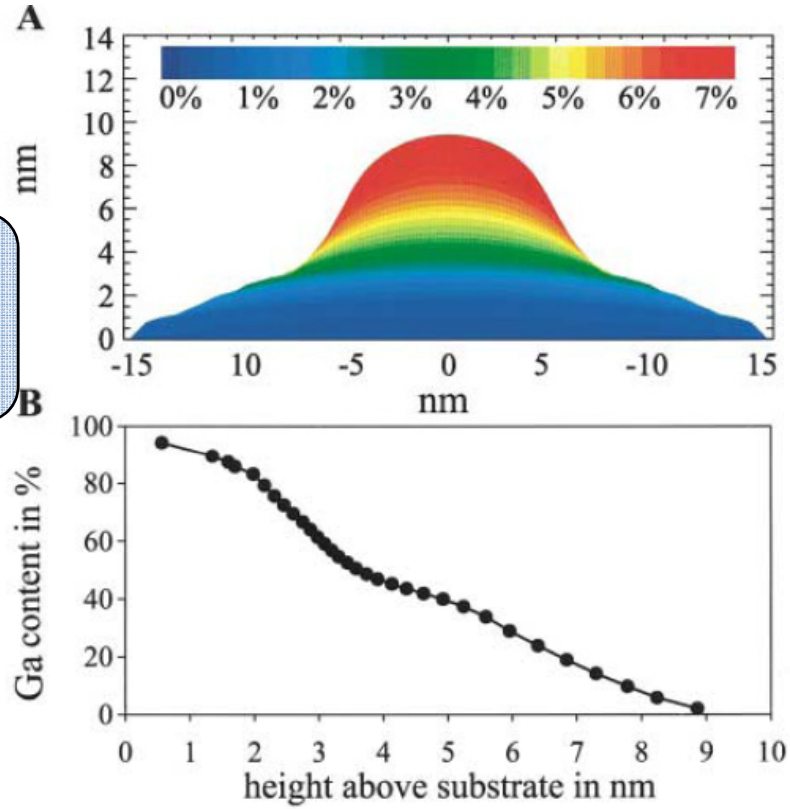

FIG. 4 (color). Experimental results for the InAs/GaAs dot system. (A) shows the deviation of lateral lattice parameter from that of GaAs, whereas in (B) the Ga-content x of the $In_{(1-x)}Ga_xAs$ alloy is displayed as a function of height above the substrate.

Material mixing ?

	Ga, 10%	Ga, 20%	Ga, 25%	0.31 eV	Exp.
m^*_{QD}/m_0	0.050	0.056	0.057	0.057	0.057 ± 0.007
$\Delta E(e)$ $\Delta E(h)$	238 245	205 217	188 151	185 206	
$e_1 - e_0$ $e_2 - e_1$	50 55	48 53	46 52	46 52	44 49
$h_0 - h_1$ $h_1 - h_2$	10 12	10 11	9 11	10 11	
E^c_{e0e0}	21.0	20.9	20.8	20.8	21.5 18.9
E^c_{e0e1}	18.1	18.0	17.9	18.0	24 13.0
E^c_{e1e1}	17.0	17.0	16.9	17.0	~18
E^c_{h0h0}	25.1	24.9	24.7	25.1	
E^c_{e0h0}	22.8	22.6	22.5	22.7	33.3
E_{ex}	1014	1075	1160	1106	1098
d_{00}	0.08	0.08	0.08	0.08	0.4 ± 0.1

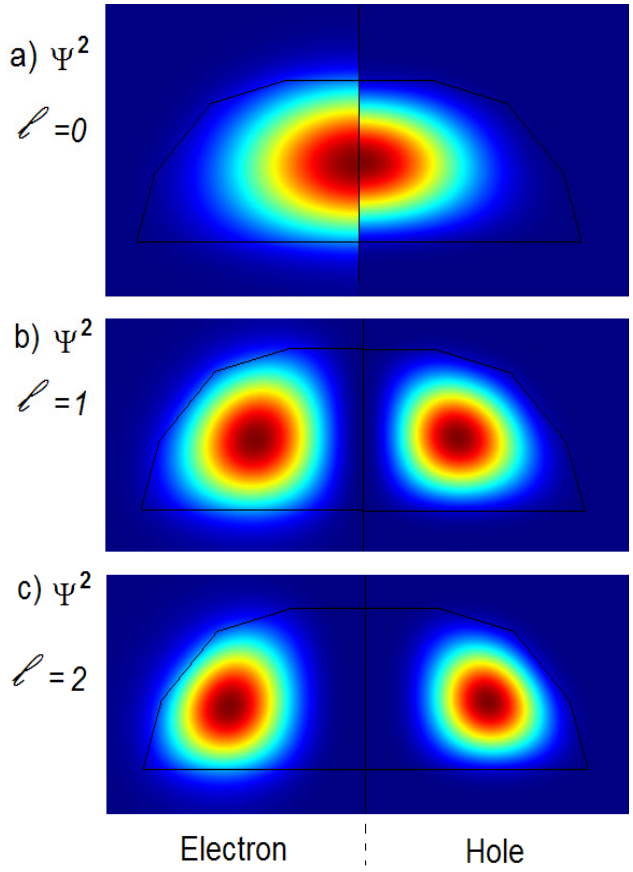

Table 1. Calculated single electron (hole) energy-level spacing e (h), electron (hole) binding energy $\Delta E(e)$ ($\Delta E(h)$), electron-electron, electron-hole and hole-hole Coulomb energies $E^c_{\alpha\beta}$ (α,β =e,h), excitonic band gap E_{ex} (in meV), exciton dipole moment d_{00} (in nm) and effective mass of the QD material for semi-ellipsoidal shaped InGaAs QDs (Ga fraction in %) embedded in GaAs. Electron (hole) energy of the ground state is measured from the GaAs conduction (valence) band. The value of the effective mass is given for p-wave electron level.

H=7 nm
B=22 nm

Ga fraction ~ 20%

Nearest Neighbor Spacing Statistics of electron level in Si QDs

Violation of 3D QD rotational symmetry

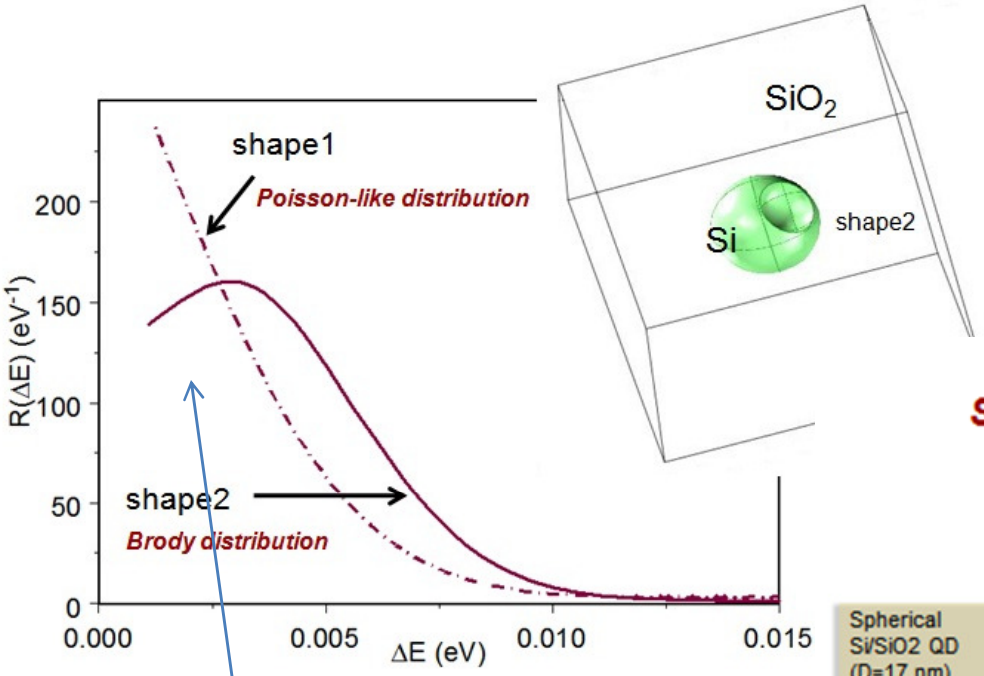

Shape1 -- initial spherical shape

Shape2 -- spherical shape with defect

Repulsion of levels near zero spacing

Distribution functions for electron neighboring levels in Si/SiO2 QD for spherical-like shape with cut. In inset the geometry of this QD are shown in 3D, the QD diameter is 17 nm. The Brody parameter beta=1.0

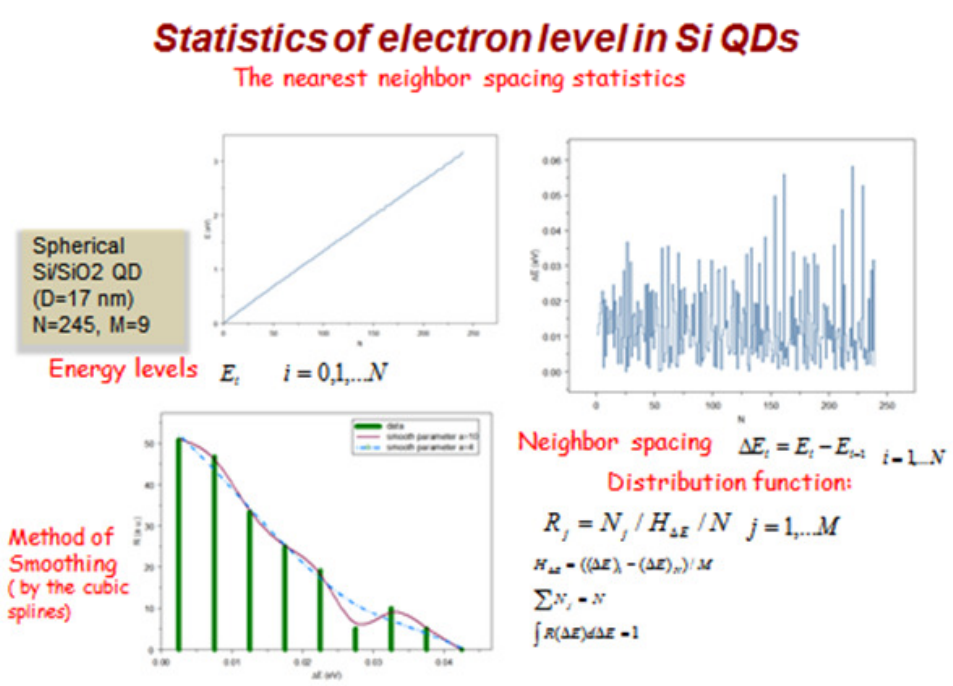

Statistics of electron level in Si QDs

3D rotational symmetry was separated

I. Filikhin, S.G. Matinyan, G. Schmid, B. Vlahovic, Physica E 42, 1979–1983 (2010).

Poisson-like distribution

Repulsion of levels near zero spacing

Brody distribution

$$R(s) = (1+\beta) b s^{\beta} \exp(-b s^{1+\beta}),$$

$$b = (\Gamma[(2+\beta)/(1+\beta)]/H)^{1+\beta}$$

T.A. Brody, *Lett. Nuovo Cimento, 7 (1973)*

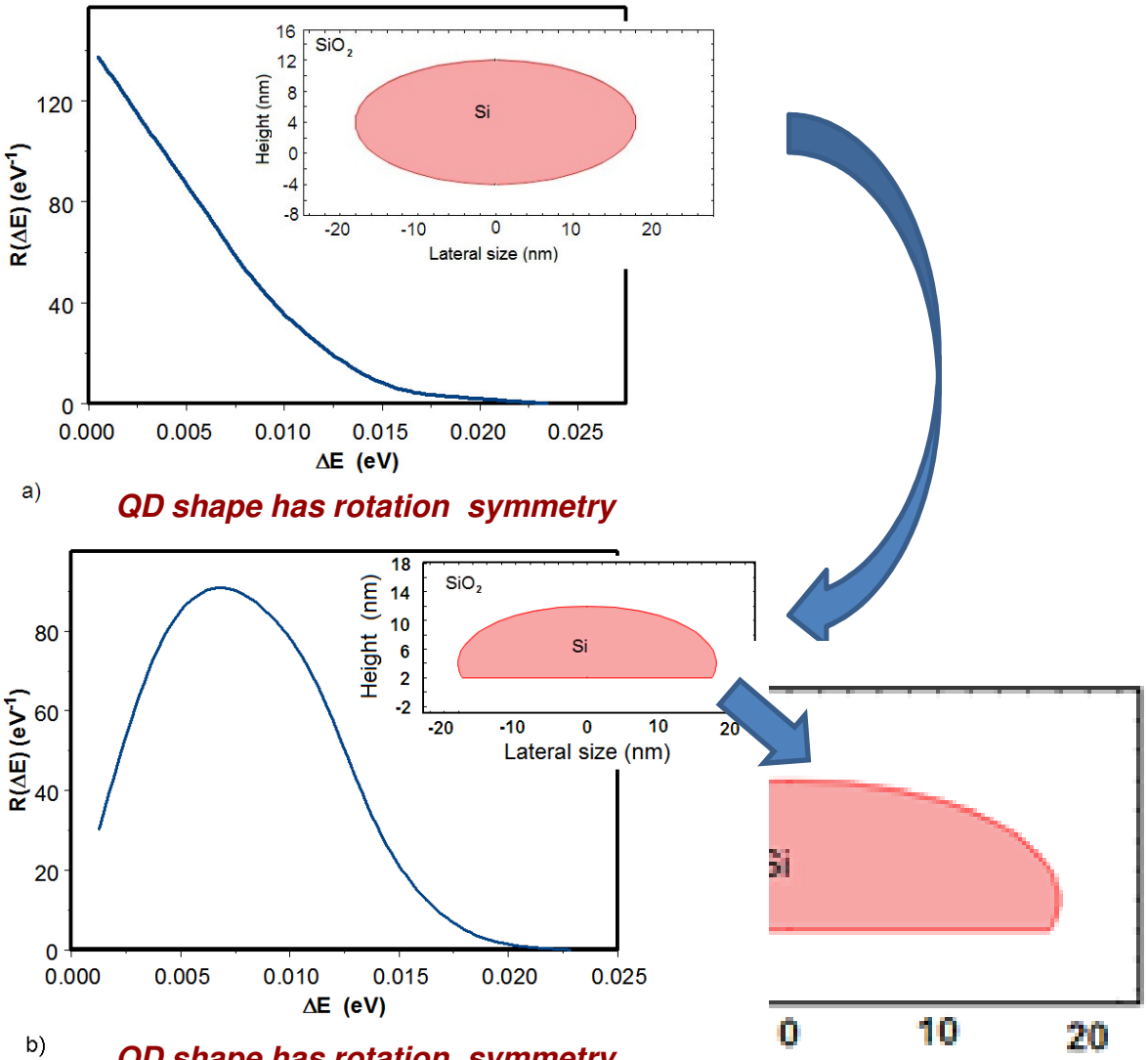

Distribution functions for electron neighboring levels in Si/SiO2 QD for different shapes:
a) ellipsoidal shape,
b) ellipsoidal like shape with cut.

Statistics of electron level in Si QDs

Violation of 3D QD rotational symmetry

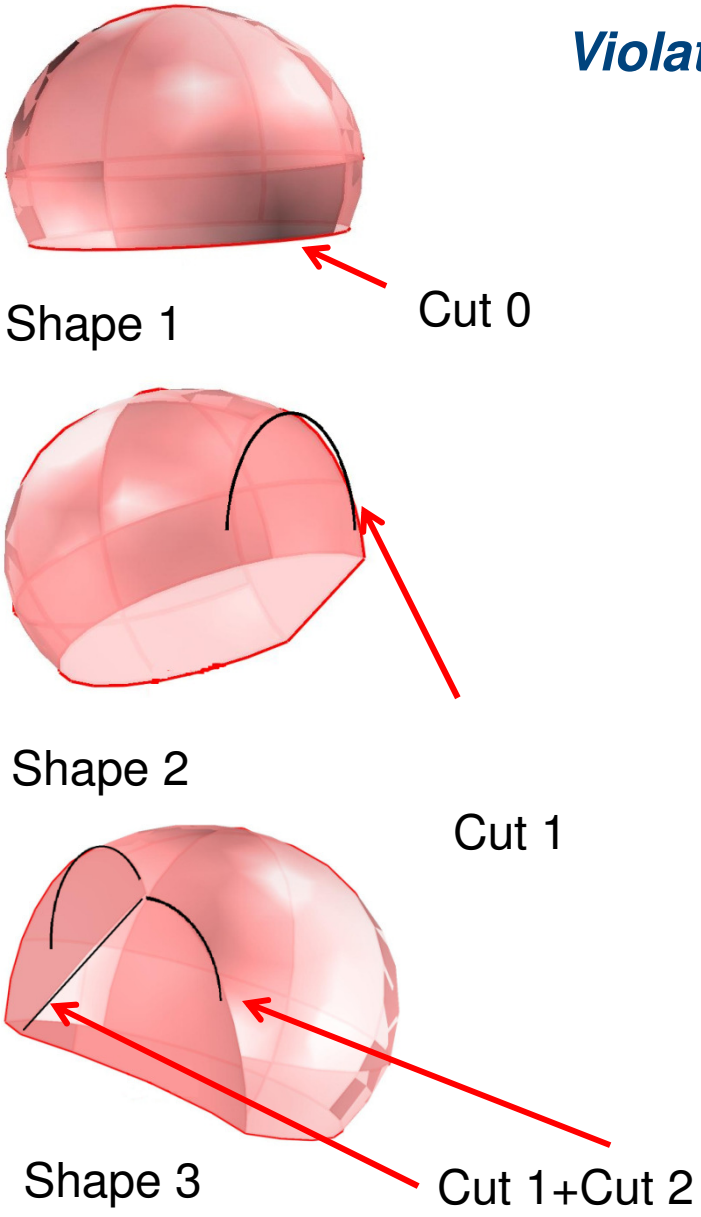

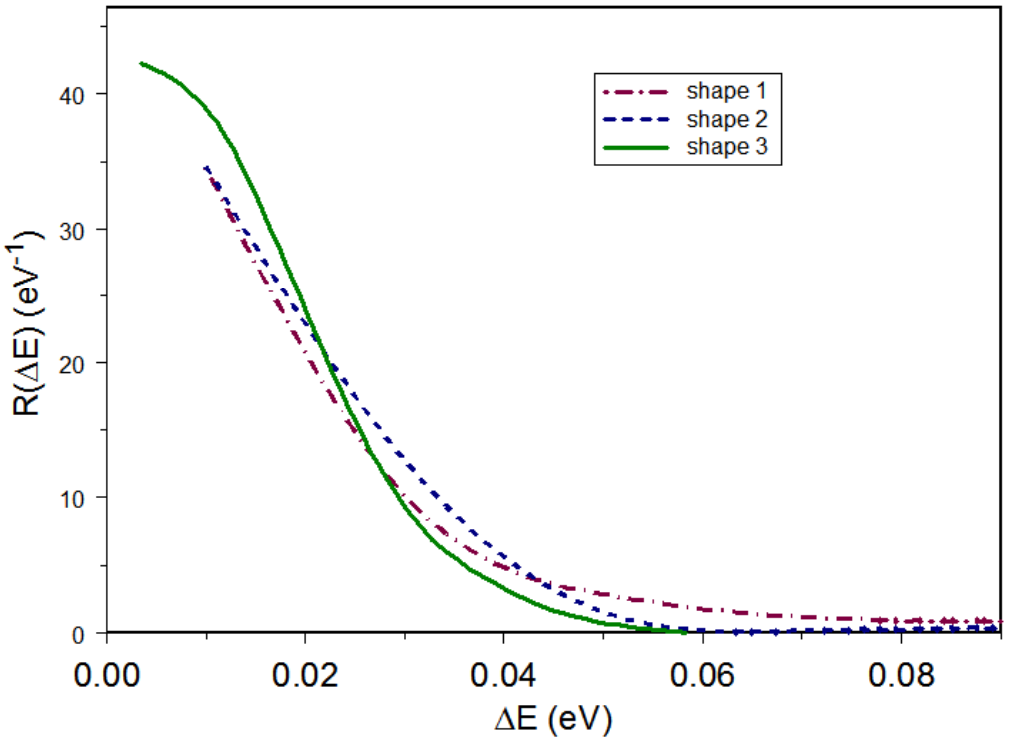

Distribution functions for electron neighboring levels in Si/SiO2 QD for semi-spherical-like shape with cut.

Statistics of electron level in Si QDs

What is the type of the statistics?

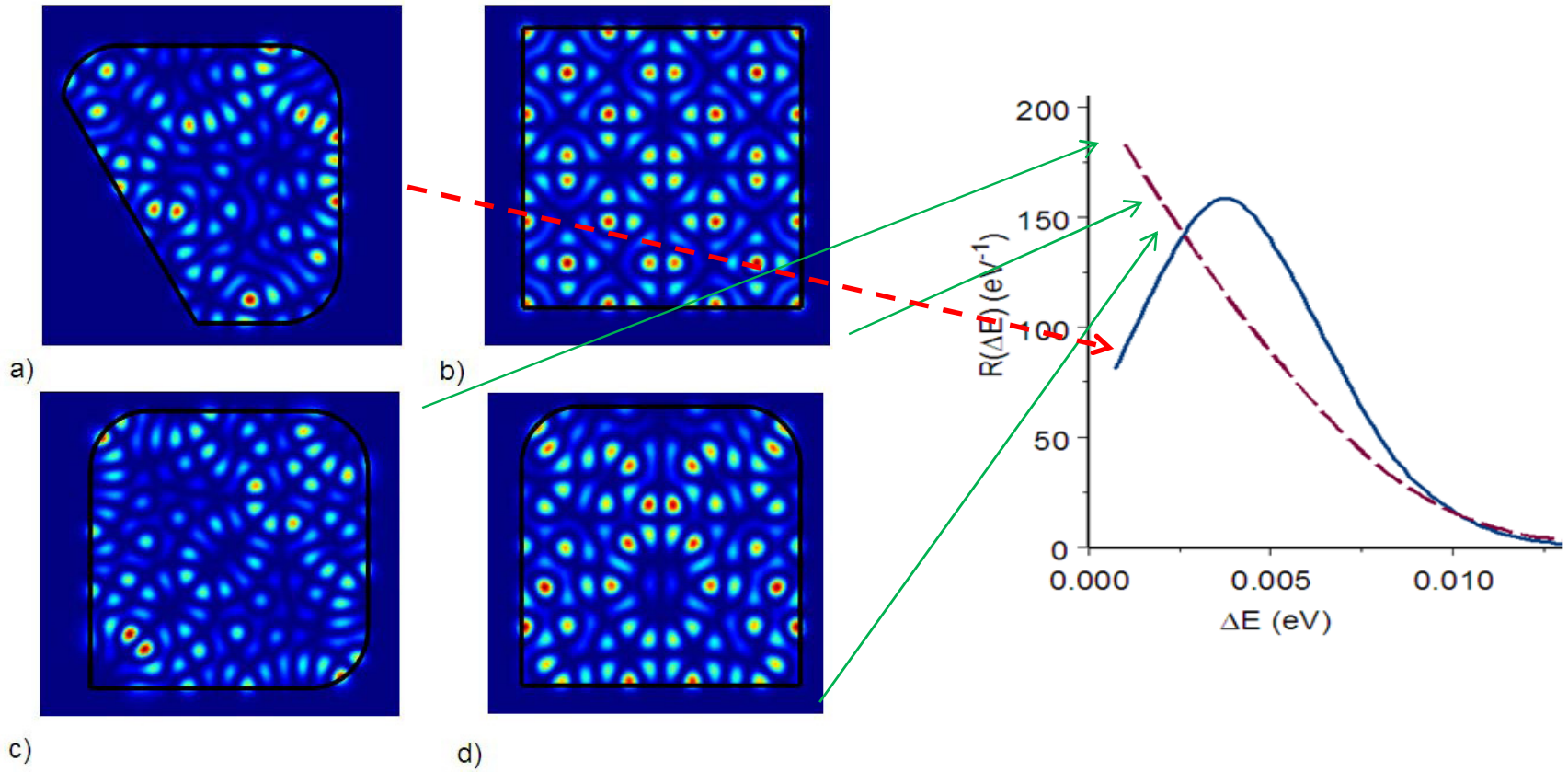

2D InAs/GaAs quantum wells: shapes and squares of wave functions for 200-th level

Neighboring Electron Level Statistics in Double Quantum Dot

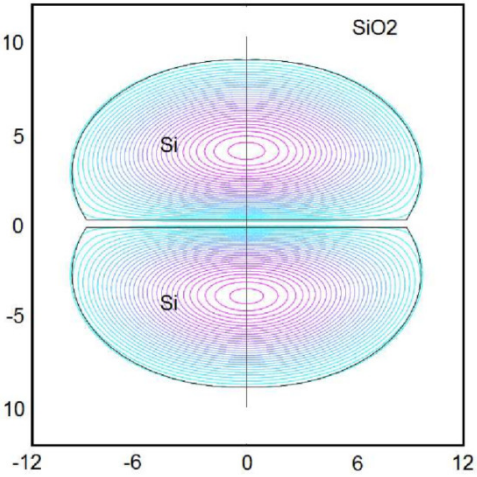

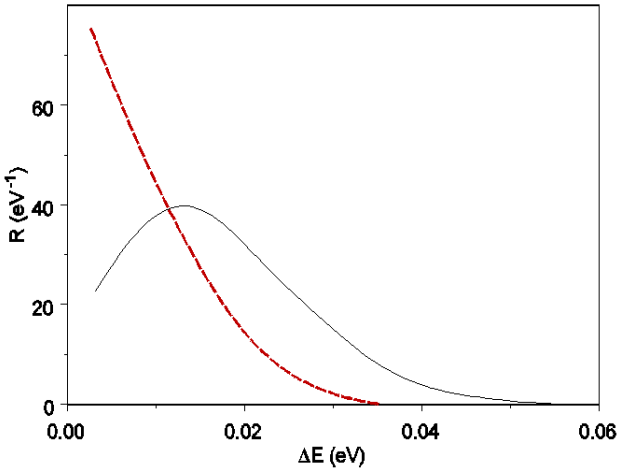

I.Filikhin, S. G. Matinyan and B. Vlahovic, arXiv:1006.3803v1, Phys. Lett. A (2010).

Distribution functions for electron neighboring levels in semispherical Si/SiO_2 single QD (fine solid line) and double QD. In the inset the cross section of DQD shape is done. The sizes are given in nm).

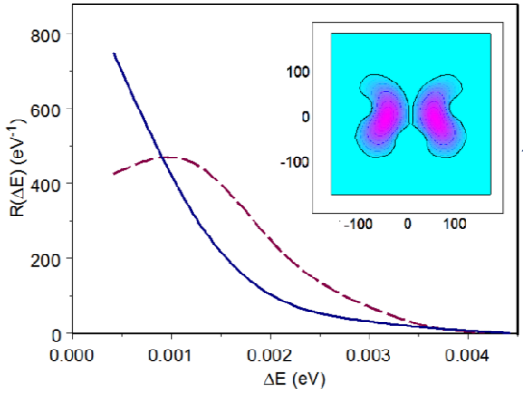

Distribution functions for energy differences of electron neighboring levels in InAs/GaAs single QW (shape taken from)(dashed line) and DQW (solid line).Shape of DQW is shown in the inset. The electron wave function of the ground state is shown by the counter plot. Data of the statistics includes about 300 first electron levels.

R.S. Whitney at al. (Phys. Rev. Lett. 102, 186802 (2009))

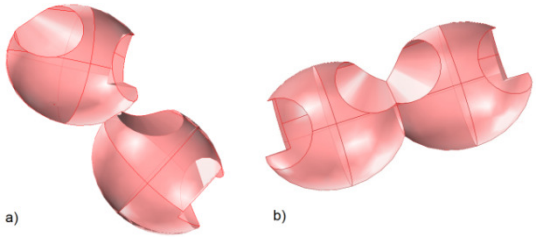

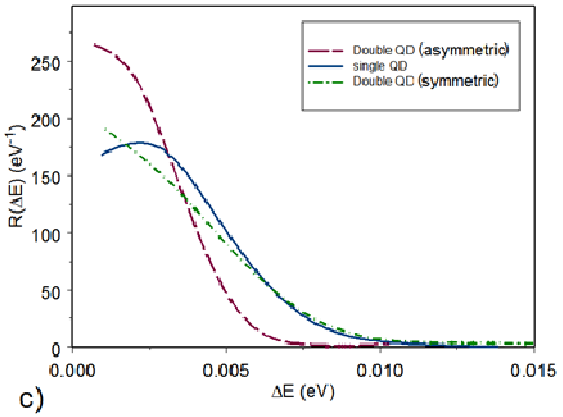

The Si/SiO_2 QD shapes have the same defects. a) Asymmetric deposition of DQD, b) symmetric deposition of DQD. c) Distribution functions for electron neighboring levels in single and double (a-b) Si/SiO_2 QDs.

Localized -Delocalized Tunneling in Double Quantum Dots

We are investigating electron localization in double quantum dots (DQD):

The tunneling means the spreading of electron wave function localized initially in one of the objects of the system into the whole double system

The localized –delocalized tunneling has a strong influence on electron transport properties through the QD array

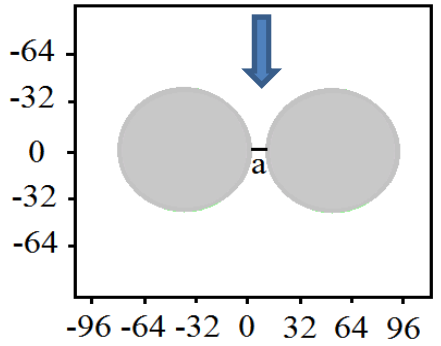

1. The effect of change of inter-dot distance (a)
2. The identical and non-identical QDs in DQD
3. A violation of symmetry of the DQD geometry and the tunneling (identical and non-identical QDs in DQD)
4. The effects electric fields to the tunneling

σ-parameter

$$\sigma = \frac{N_{n,1} - N_{n,2}}{N_{n,1} + N_{n,2}}, \text{ with the range of } [-1,1]$$

$$N_{n,\gamma} = \iint_{\Omega_\gamma} |\Phi_n(x,y)|^2 \, dxdy, \text{ where } \Phi_n(\rho,z) \text{ is wave function of electron,}$$

Ω_γ (γ =1, 2) are dictated by the QD shapes

Localization and Delocalization in the system of two quantum dots

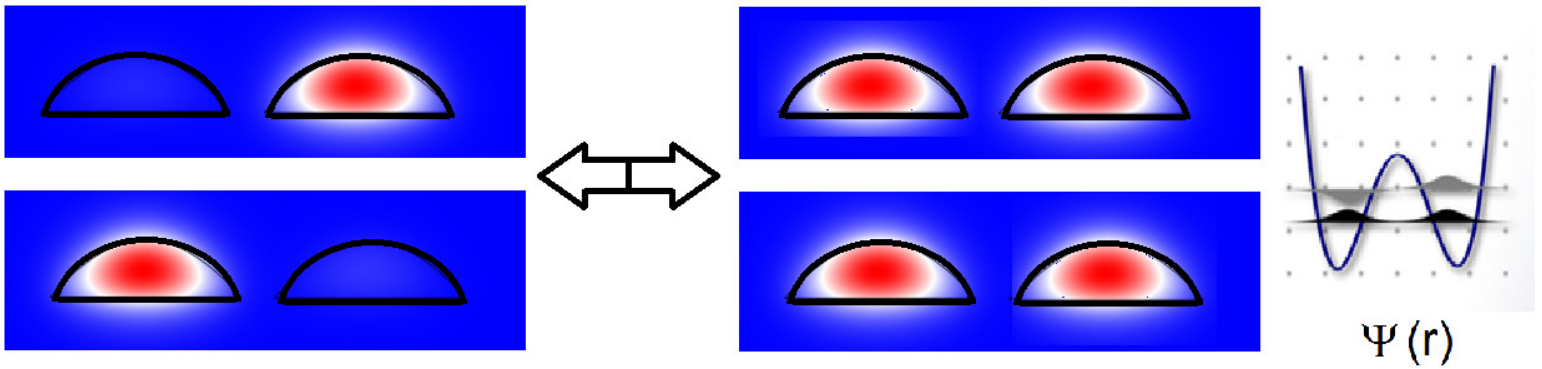

$\Psi(\mathbf{r})$ - wave function of a single electron

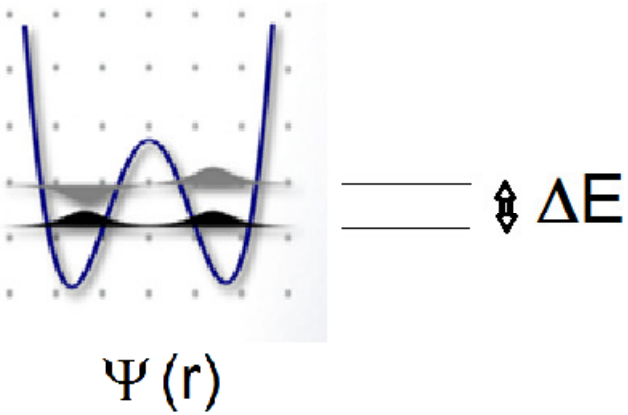

Overlapping wave functions of left (L) and right (R) quantum dots :

$$\Delta E \sim \sum_{n=1,2} \int \Psi^n{}_L(x,y) V_c(x,y) \Psi^n{}_R(x,y) dxdy$$

One dimensional double quantum well:

O. Manasreh, Semiconductor Heterojunctions and Nanostructures, McGraw-Hill 2005 pp. 78-80.

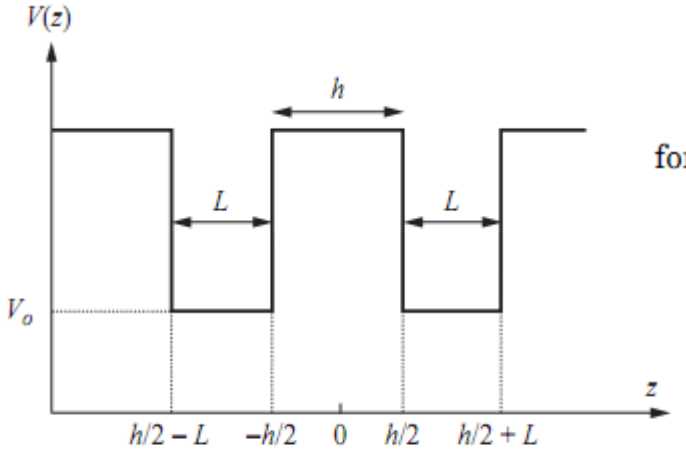

Figure 2.26 Identical double potential wells separated by a potential barrier of width h.

$$\mathbf{H} = T + V_1(z) + V_2(z)$$

for the isolated wells

$$[T + V_1(z)]\chi_1(z) = E_1\chi_1(z)$$

$$[T + V_2(z)]\chi_2(z) = E_1\chi_2(z)$$

$$\psi(z) = A_1\chi_1(z) + A_2\chi_2(z)$$

$$E = E_1 + \frac{\overline{V}_1 \pm \overline{V}_{12}}{1 \pm S}$$

$$S = \langle \chi_1 \mid \chi_2 \rangle$$

$$\overline{V}_1 = \langle \chi_1 | V_2(z) | \chi_1 \rangle = \langle \chi_2 | V_1(z) | \chi_2 \rangle$$

$$\overline{V}_{12} = \langle \chi_1 | V_1(z) | \chi_2 \rangle = \langle \chi_2 | V_2(z) | \chi_1 \rangle$$

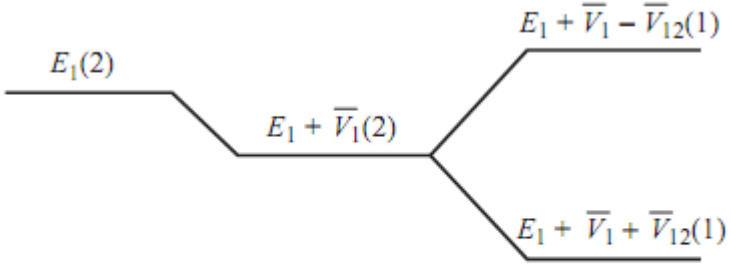

Figure 2.27 Shifting and lifting the degeneracy of the two ground-state isolated quantum wells due to the coupling between the wells. The numbers in parentheses reflect the degeneracy [see Bastard (1988) for additional details].

Effective potential model for InAs/GaAs heterostructures*

- ***kp***-perturbation theory [Luttinger J. M. and Kohn W. Phys. Rev. **97**, 869 (1955) in a single sub-band approach

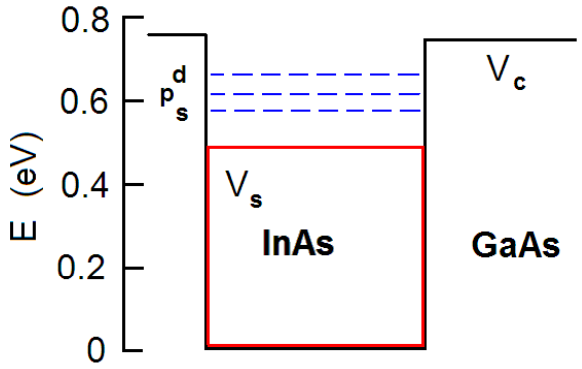

$$\left(H_{kp}+V_c(\mathbf{r})+V_s(\mathbf{r})\right)\Psi(\mathbf{r})=E\Psi(\mathbf{r}),$$

$H_{kp}=-\nabla\frac{\hbar^2}{2m^*(\mathbf{r})}\nabla$ - the one band ***kp*** Hamiltonian operator

$V_c(\mathbf{r})$ - the band gap potential: $V_c(\mathbf{r})=\begin{cases}0, & \in QD,\\ V_c, & r\notin QD,\end{cases}$

$m^*(\mathbf{r})$ - the electron effective mass: $m^*(\mathbf{r})=\begin{cases}m^*_{QR}, & r\in QD,\\ m^*_{Substrate}, & r\in Substrate,\end{cases}$

$V_s(r)$ is the effective potential simulating the strain effect

V_c =0.594 eV $V_s(\mathbf{r})$ =0.21 eV

$m_1=0.024\,m_0$ and $m_2=0.067\,m_0$

InAs GaAs

The Ben-Daniel-Duke boundary conditions are used on the interface of the material of QD and substrate.

*Filikhin, I. / Suslov, V.M. / Wu, M. / Vlahovic, B. InGaAs/GaAs quantum dots within an effective approach, *Physica E: Low-dimensional Systems and Nanostructures*, 41, 1358-1363, 2009.

Two identical quantum dots

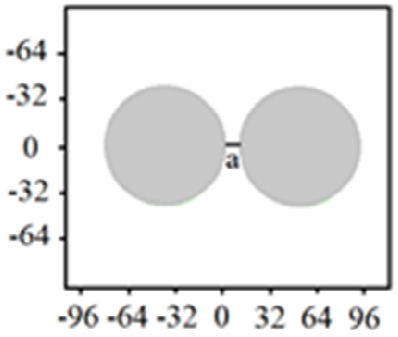

Lateral **InAs/GaAs** DQD; sizes is given in nm

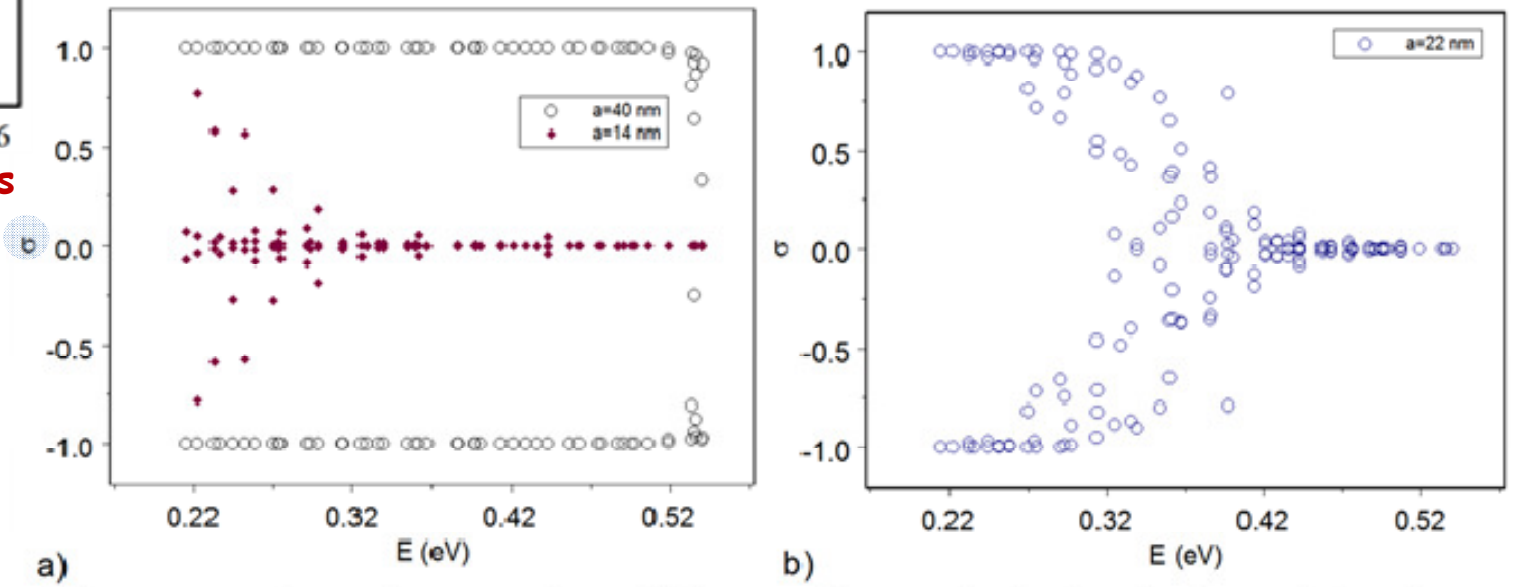

The parameter σ for energies of the confinement single electron states in InAs/GaAs DQD. Inter-dot distances are a) 14 nm, 40 nm; b) 22 nm.

inter-dot distance:

a=40 nm
localized state

a=14 nm
delocalized state

Tunneling rate (overlapping of the wave functions)

$$\Delta E \sim \sum_{n=1,2} \int \Psi^n{}_L(x,y) V_c(x,y) \Psi^n{}_R(x,y) dxdy$$

is large for upper states of the spectrum

There are three parts of the spectrum: separated QDs region (no tunneled states), weak coupling region (intermediate) and the strong coupling region (tunneled states)

Two identical quantum dots

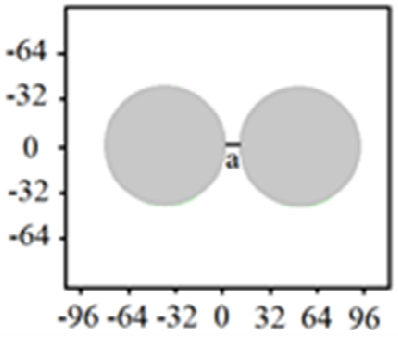

Lateral **InAs/GaAs** DQD; sizes is given in nm

Localized levels

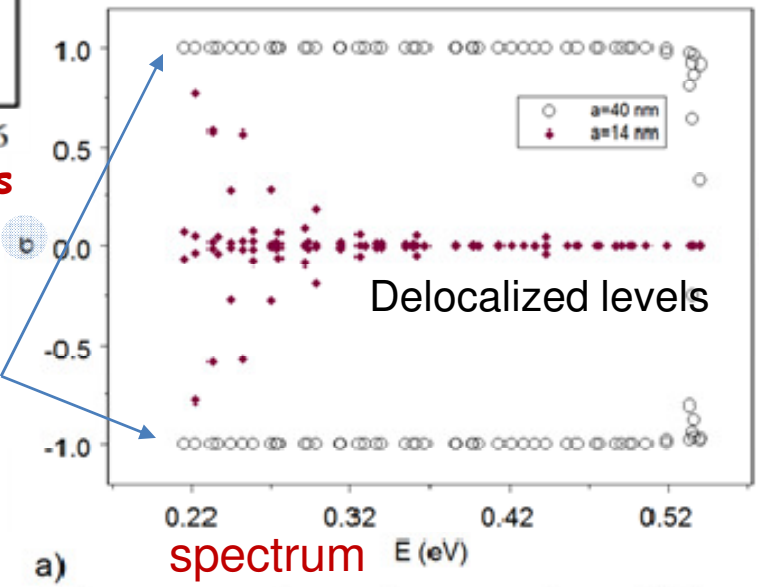

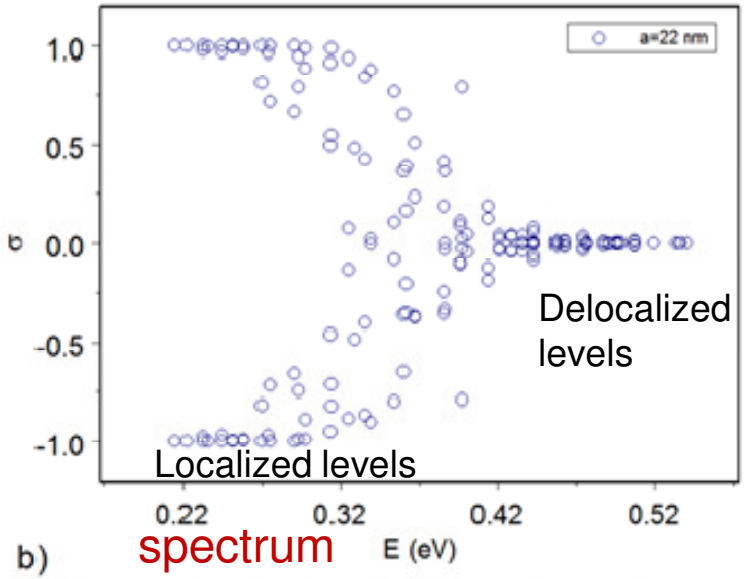

The parameter σ for energies of the confinement single electron states in InAs/GaAs DQD. Inter-dot distances are a) 14 nm, 40 nm; b) 22 nm.

inter-dot distance:

a=40 nm
localized state

a=14 nm
delocalized state

To describe tunneling of a single electron in doublet quantum objects we made some definitions. Probability of localization of electron into region Ω_γ (γ =1,2) is defined by the following formula $N_{n,\gamma} = \iint_{\Omega_\gamma} |\Phi_n(x,y)|^2 \, dxdy$, where $\Phi_n(\rho,z)$ is wave function of electron, n is the number of the state. Ω_γ (γ=1,2) are conceited with the QD shapes. Let us define as tunneling measure parameter σ equal $\sigma = \dfrac{N_{n,1} - N_{n,2}}{N_{n,1} + N_{n,2}}$ with the range [-1,1]. Obviously, when $\sigma = 0$, the electron will be in QD1 (Ω_1) or in QD2 (Ω_2) with equal probability (here we assume, that the QD1 and QD2 have the same shape). This situation is possible when an electron is tunneling between QD1 and QD2. The case $\sigma = 1$ ($\sigma = -1$) is possible when a single election is strong located in QD1 (QD2).

Two non identical quantum dots

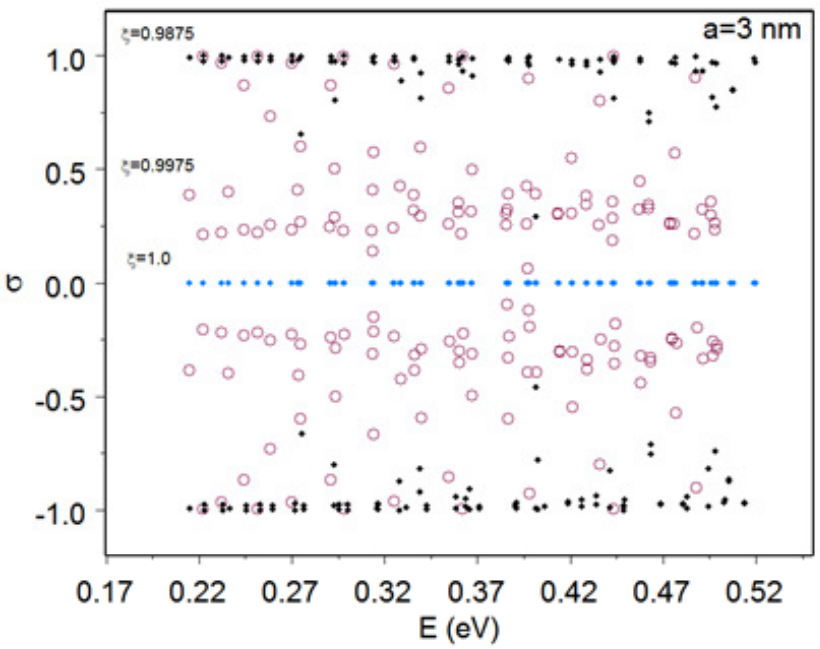

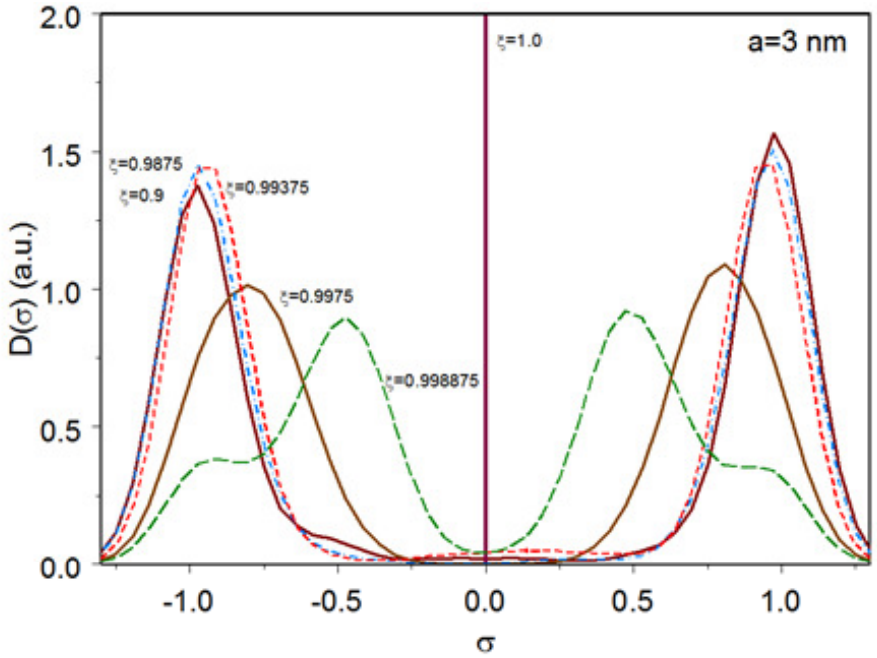

a) b)

a) Parameter σ for different coefficient of asymmetry in asymmetric DQD with R_1 =40 nm and $R_2 = \xi R_1$.

b) Density functions of the σ parameter.

fixed inter-dot distance a=3 nm

ξ=0.9875	strong localization
ξ=0.9975	weak localization
ξ=1.0	delocalized state

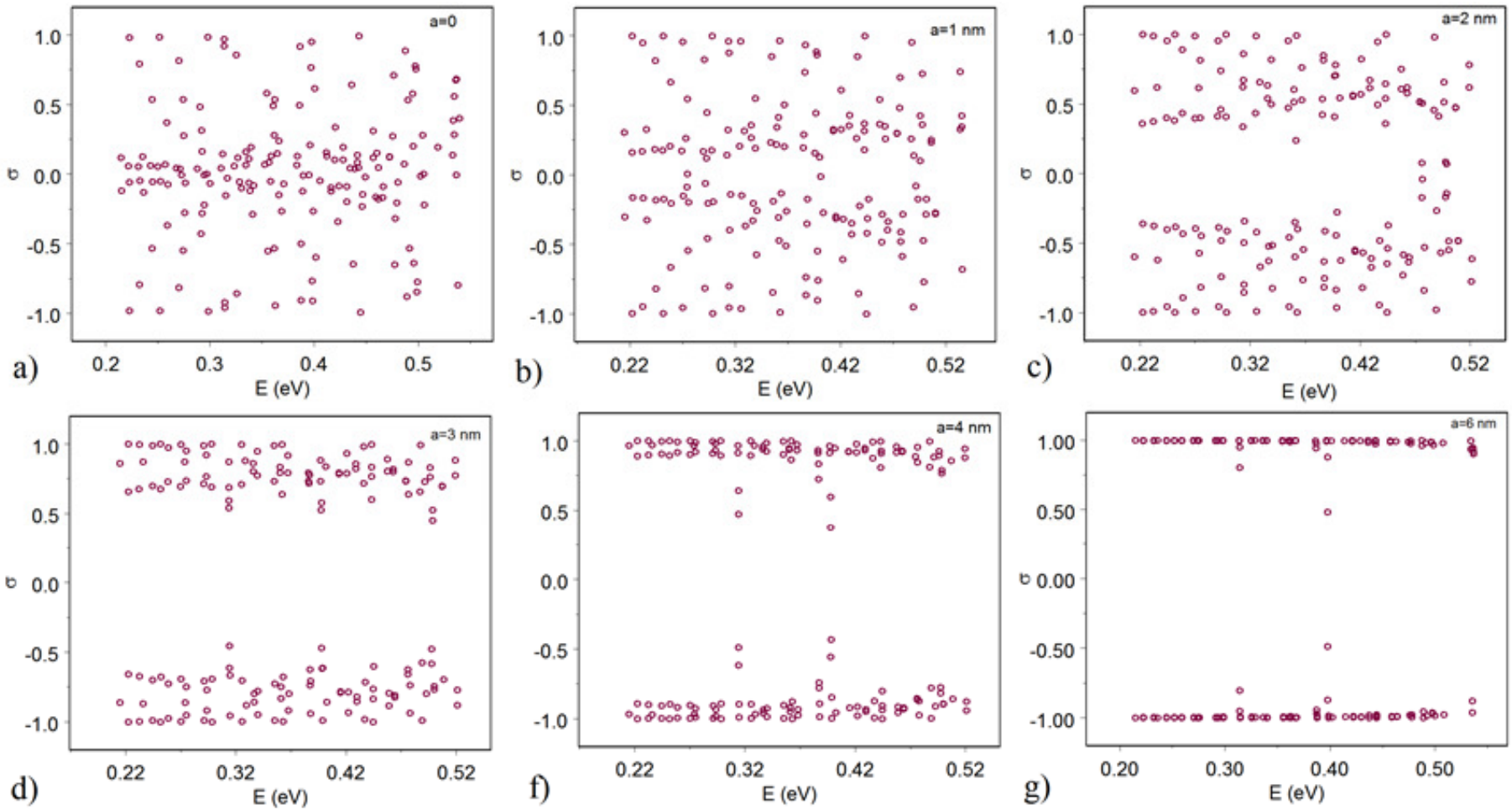

The σ-parameter for the asymmetric DQD with R_1 =40 nm and R_2 =39.9 nm for different inter-dot distances a.

Two types of the tunneling 1) for identical 2) for non-identical DQDs: regular and "chaotic".

I. Filikhin, S. G. Matinyan, and B. Vlahovic, Electron tunneling in double quantum dots and rings, J*ournal of Physics: Conference Series* 393 (2012) 012012.

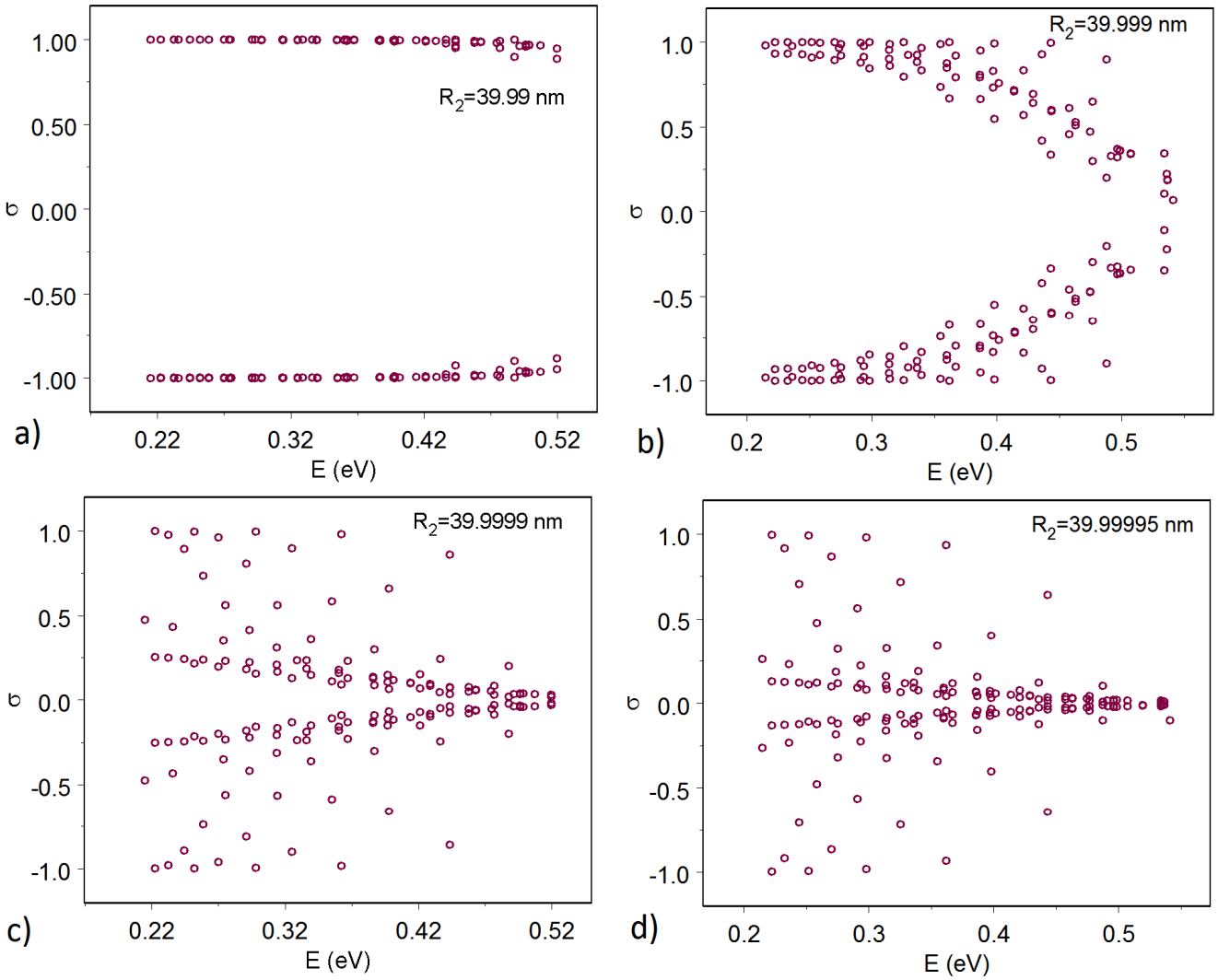

σ-parameter for the asymmetric DQD with a=10 nm for several values of the asymmetry ξ

$$R_2 = \xi R_1 .$$

3D Semi-ellipsoidal shaped InAs/GaAs DQD

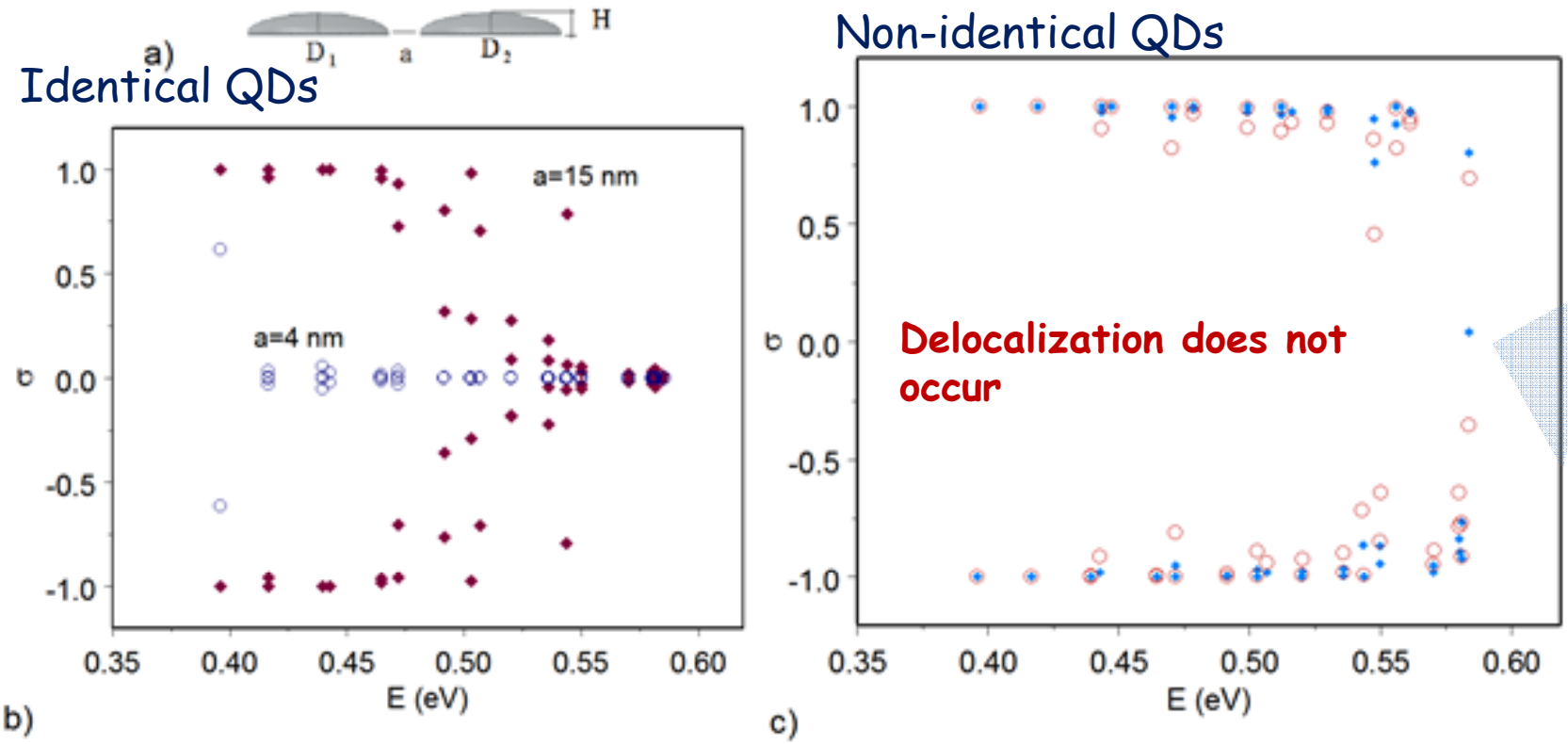

a) Cross section of 3D semi-ellipsoidal shaped lateral DQD.

b) σ-parameter for 3D InGaAs/GaAs DQD with $R_1 = R_2 = 20$ nm calculated for energies of single electron spectrum for different inter-dot distances a (shown in the figure).

c) σ-parameter for 3D InGaAs/GaAs DQD with $R_1 = 20$ nm and $R_2 = 19$ nm for different inter-dot distances a: solid diamonds for $a = 1$ nm, open circles for $a = 0$.

Identical QDs

For inter-dot distance $4 < a < 15$ nm
the transformation occurs from localized state to delocalization state

The symmetry violation which is not related to volume area differences

Lateral DQR with non-concentric deposition

The lateral deposited QRs in DQR. Δx is the shift of inner circle in upper QR.

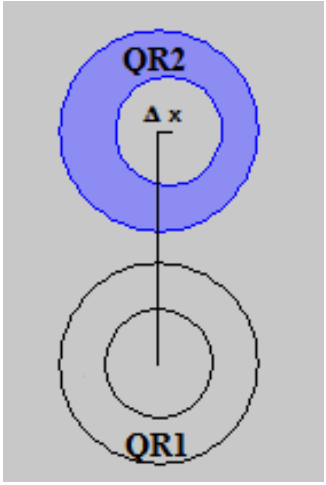

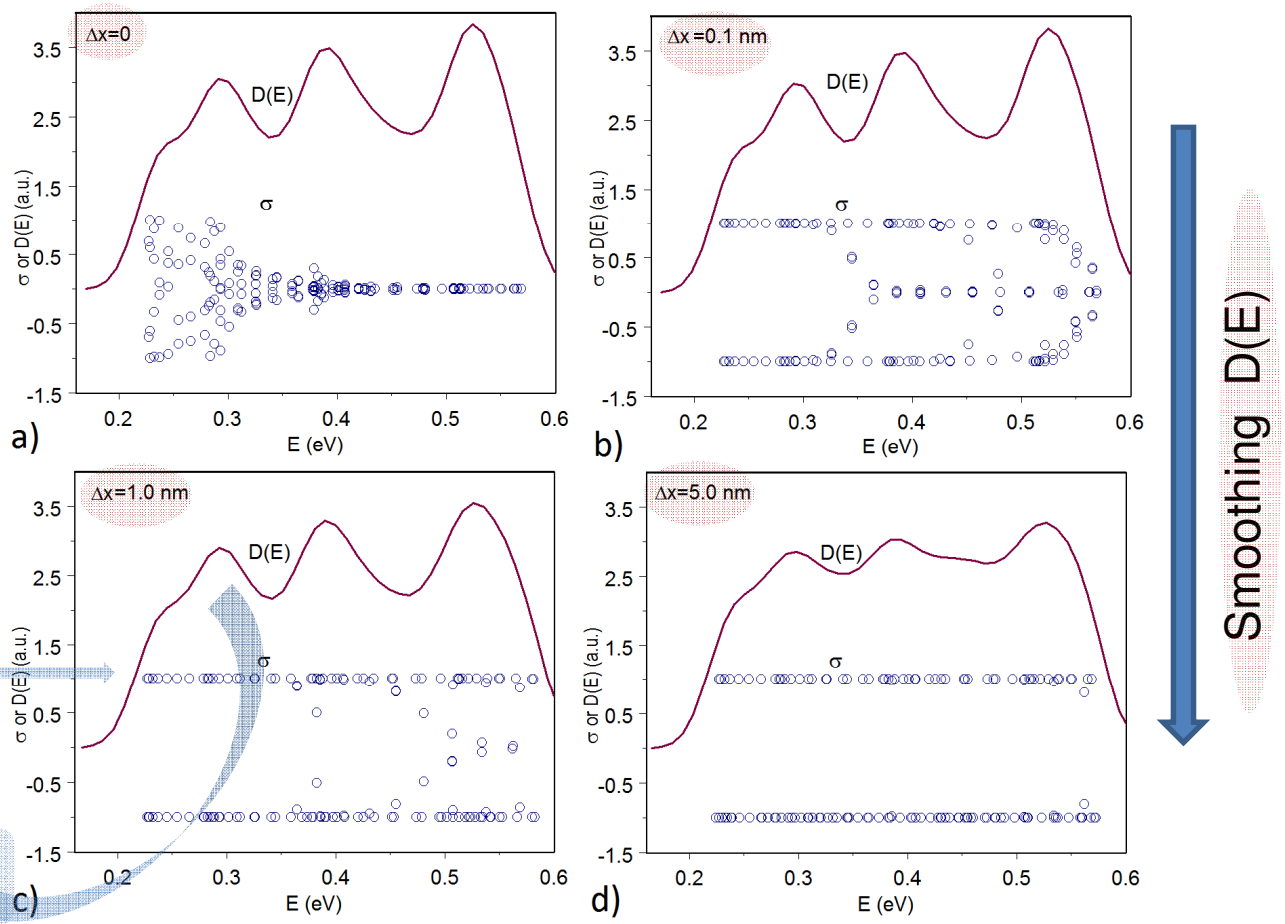

Structure of the spectrum of the symmetric ring QR1

$$E_{n,l} \sim \hbar / 2m^{*}(n^2 / W^2 + l^2 / R^2)$$

$W << R$ where W is the width of the QR.

The local maximums correspond to the Low-lying levels of different n-bands

σ-parameter and density function in InGaAs/GaAs DQR along electron spectrum for different shifts Δx a) 0 b) 0.1nm c) 1nm d) 5nm

The violation of symmetry in the single ring (upper ring)

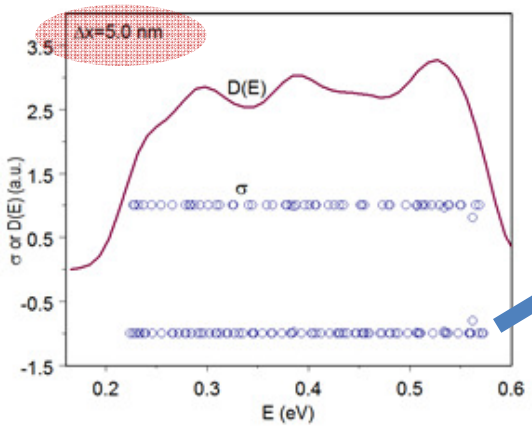

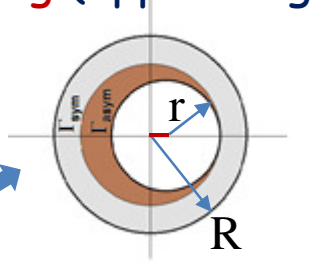

outer radius is R
inner radius is r

Δx<r → weak symmetry violation

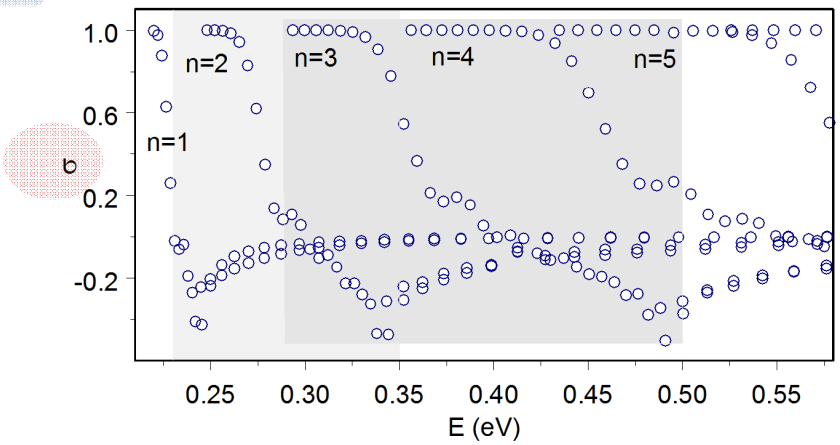

Δx>r → Strong symmetry violation

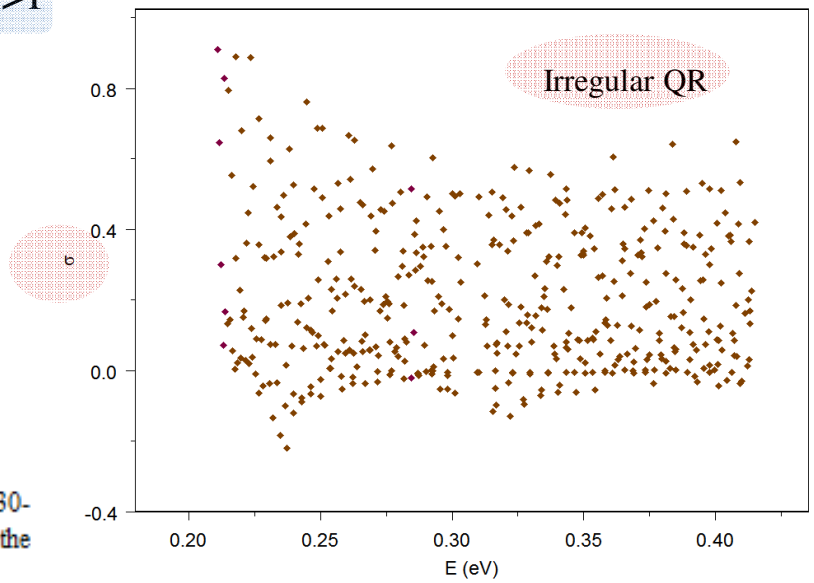

The parameter σ and the single electron spectrum of the InAs/GaAs QR with $d=R-(r+\delta)$=1.5(30-(19+4)) nm. The bands are enumerated by n=1, 2, 3, 4. The shadowing energy intervals marks the "beach" regions for the n=1 and n=2 bands.

When Δx increases => wave function each level becomes a mix of the functions with different symmetries.

Special size and form or N-dot Quantum dot molecules

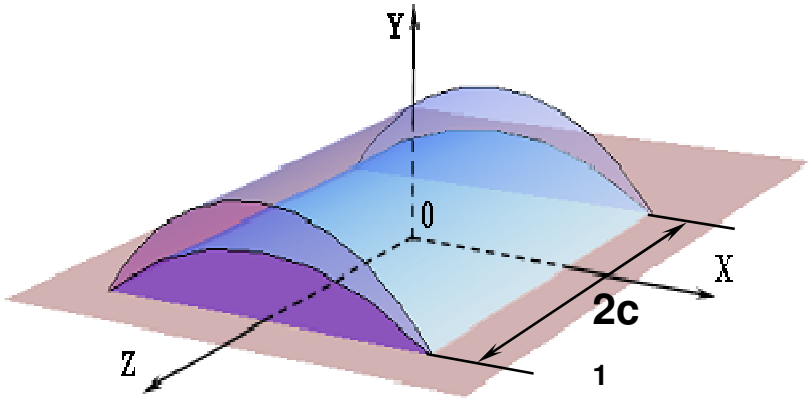

Cylindrical QD with falciform cross-section

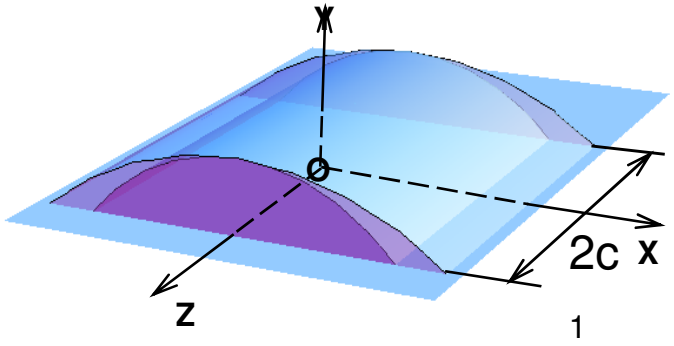

Cylindrical QD with thin lens shaped cross-section

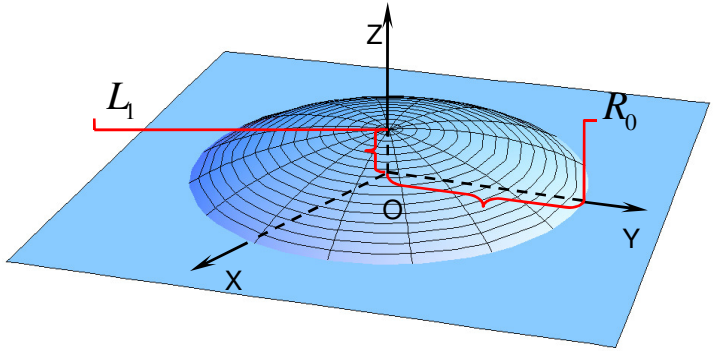

Ellipsoidal quantum lens

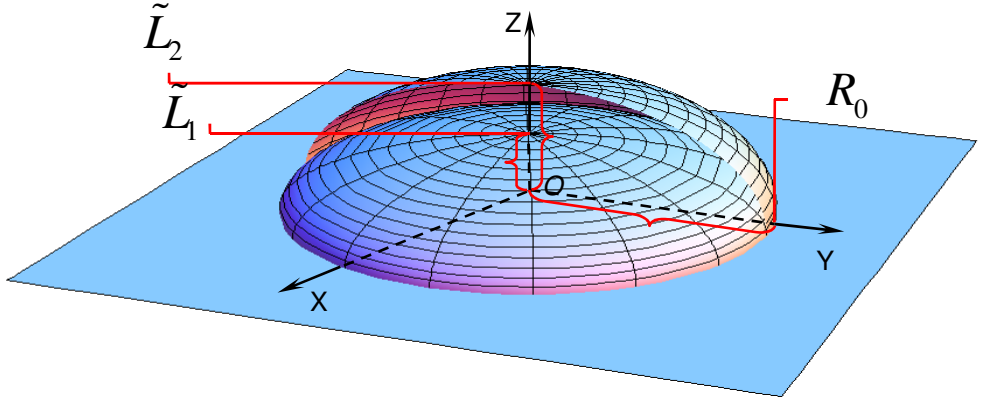

Coated ellipsoidal quantum lens

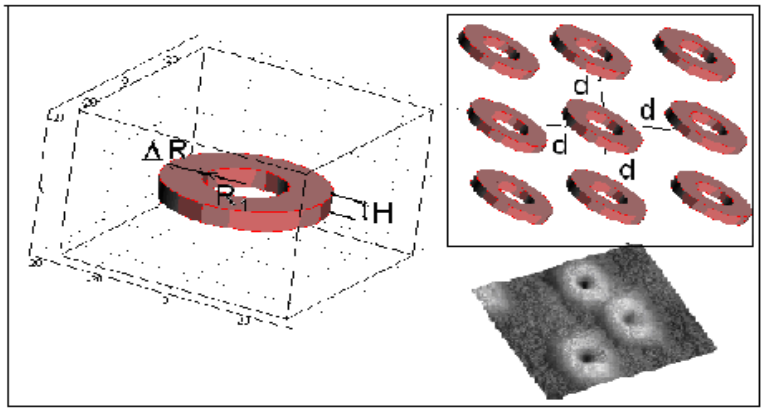
ΔR
R1
H
d
d
d
d

a)

b)

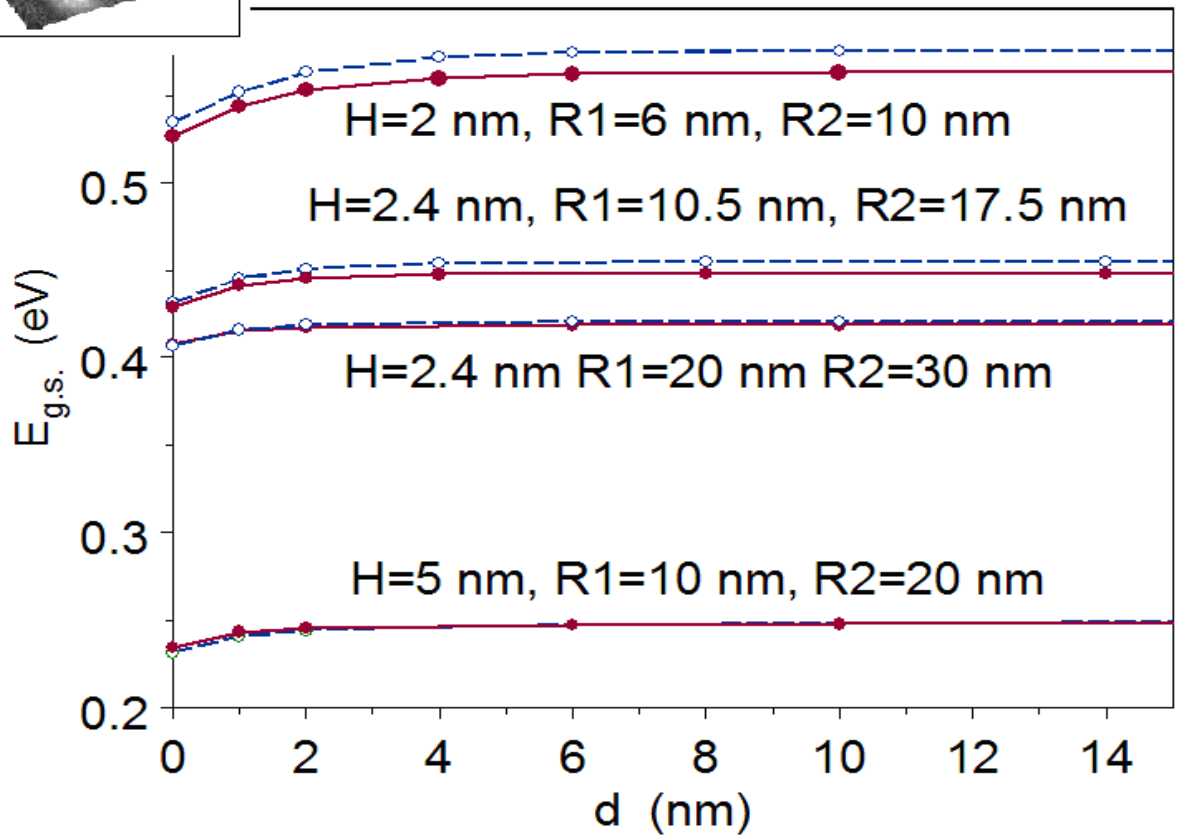
H=2 nm, R1=6 nm, R2=10 nm
H=2.4 nm, R1=10.5 nm, R2=17.5 nm
H=2.4 nm R1=20 nm R2=30 nm
H=5 nm, R1=10 nm, R2=20 nm
E g.s. (eV)
0.5
0.4
0.3
0.2
0
2
4
6
8
10
12
14
d (nm)

Fig. 7

N-dot Quantum dot molecules

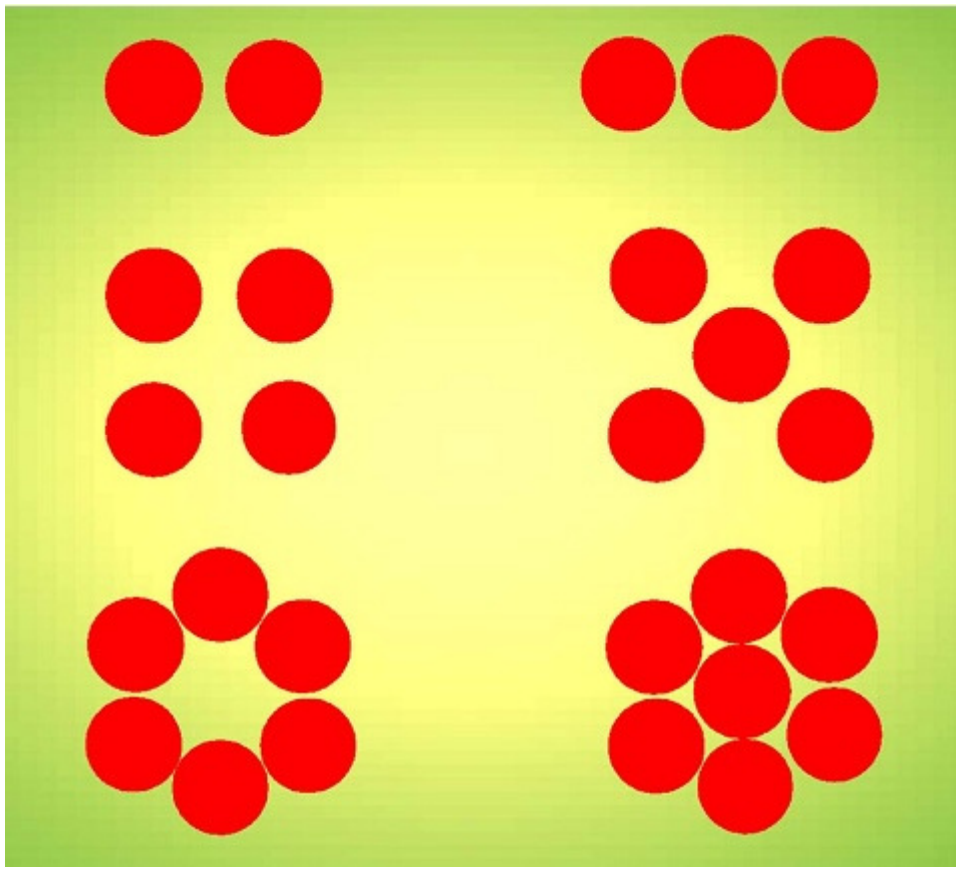

N-dot Quantum dot molecules
Experimental Data

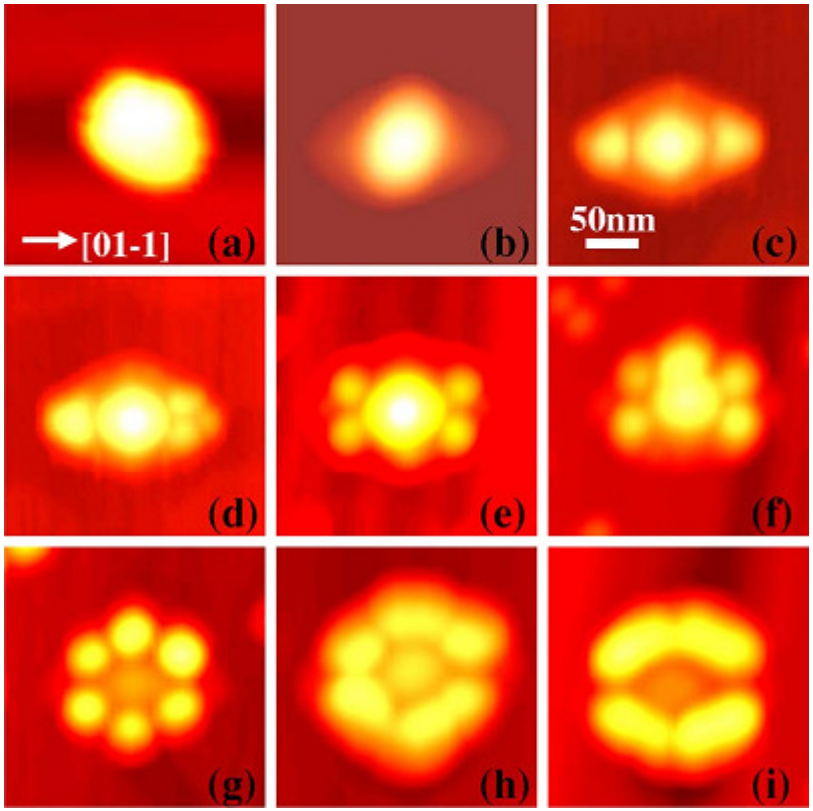

J. H. Lee, Zh. M. Wang, N. W. Strom, Yu. I. Mazur, and G. J.Salamo.
APPLIED PHYSICS LETTERS 89, 202101(2006)

Quantum dot molecules (4 Dots)
Experimental Data

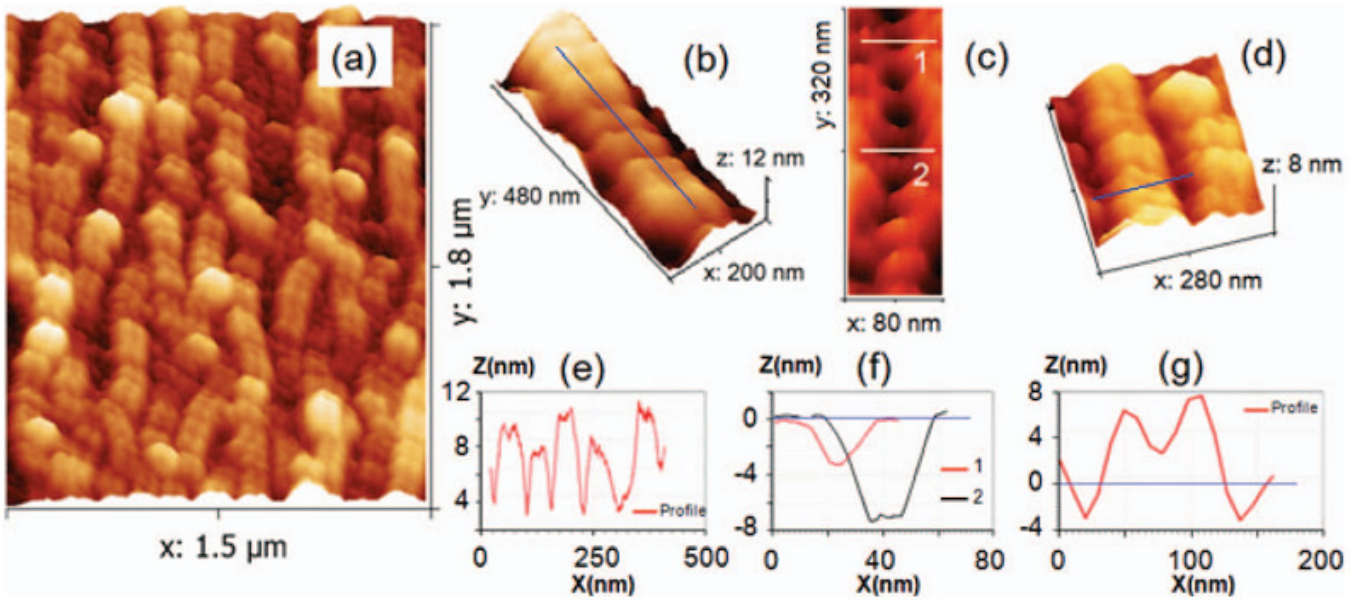

K. M. Gambaryan and V. M. Aroutiounian.

AIP Advances 3, 052108 (2013)

Quantum dot molecules (4 or 5 Dots)

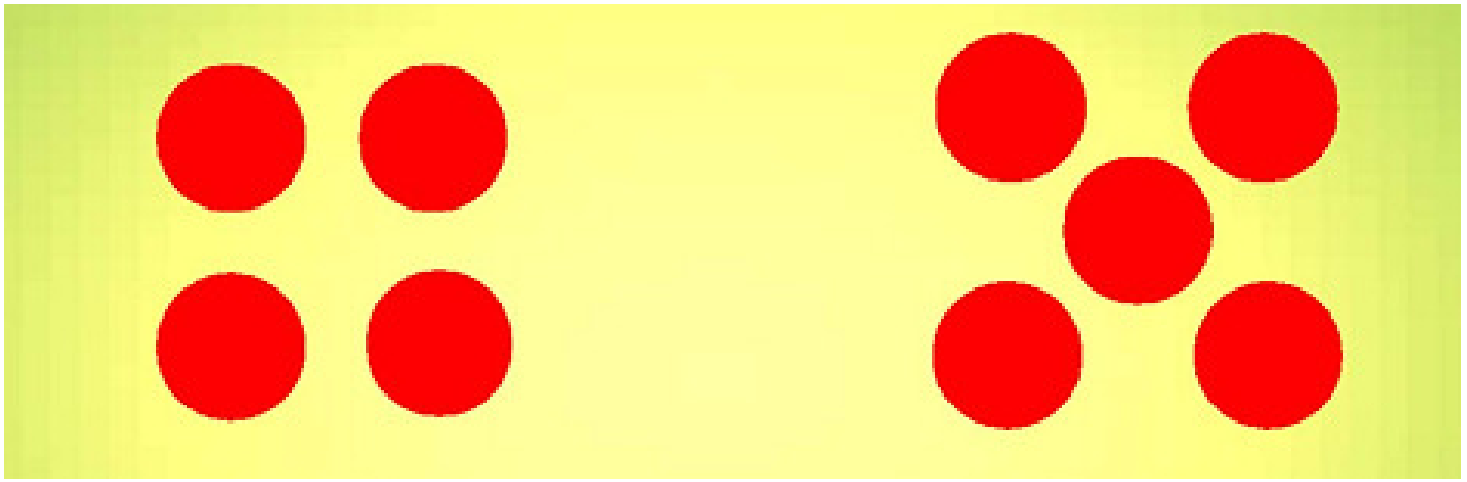

K. G. Dvoyan, E. M. Kazaryan, A. A. Tshantshapanyan, Zh. M. Wang, and G. J. Salamo. “Electronic states and light absorption in quantum dot molecule”. **Appl. Phys. Lett. 98**, 203109 (2011); doi:10.1063/1.3592258.

Motion of electron in 4 – dot quantum dot molecule

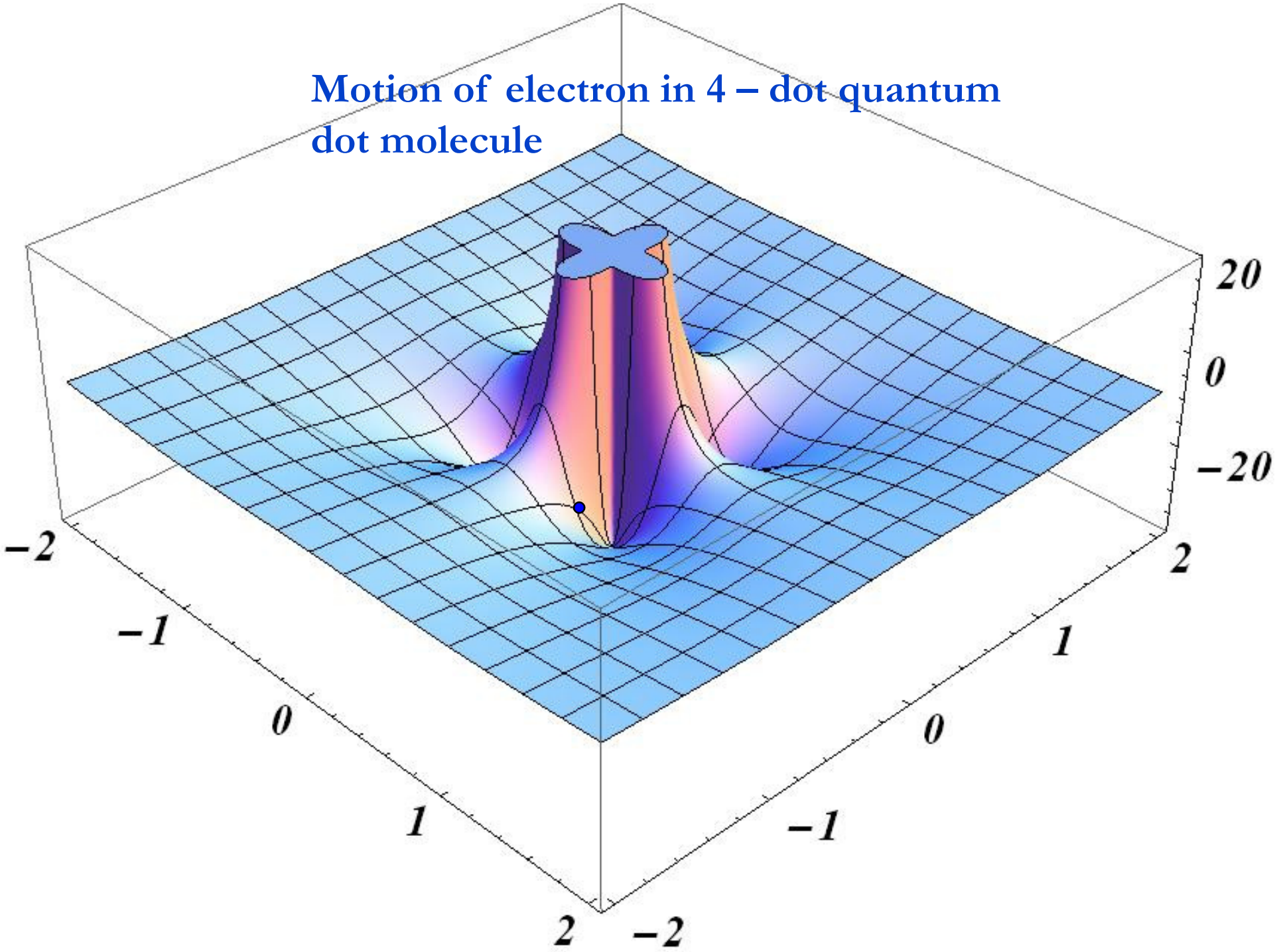

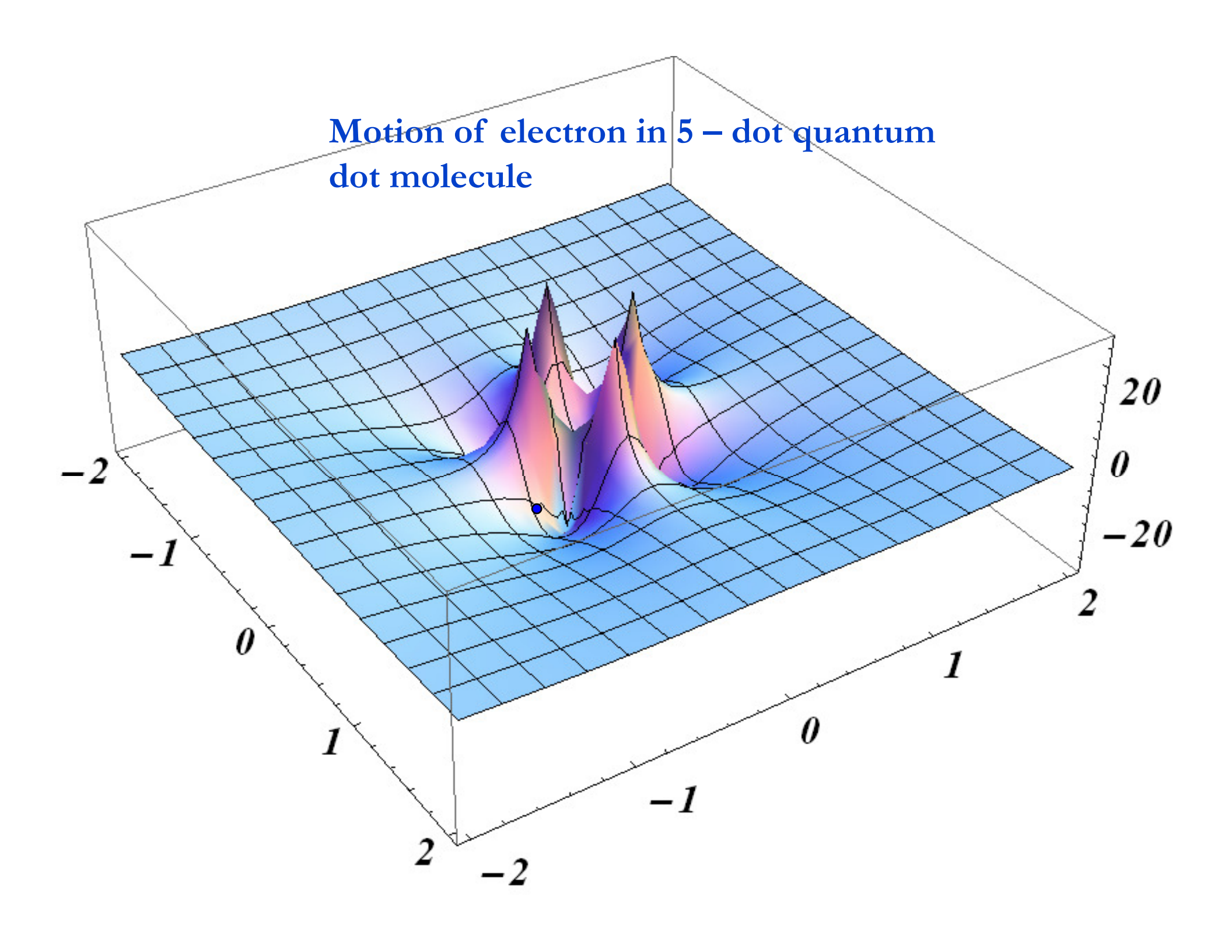
Motion of electron in 5 – dot quantum dot molecule
−2
−1
0
1
2
−2
−1
0
1
2
20
0
−20

The symmetry violation which is not related to volume area differences: Electric field effect

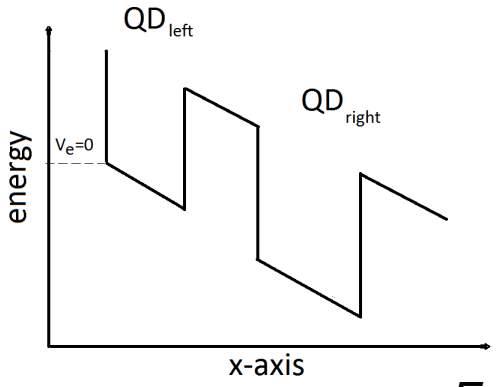

Identical lateral IsAs/GaAs QDs

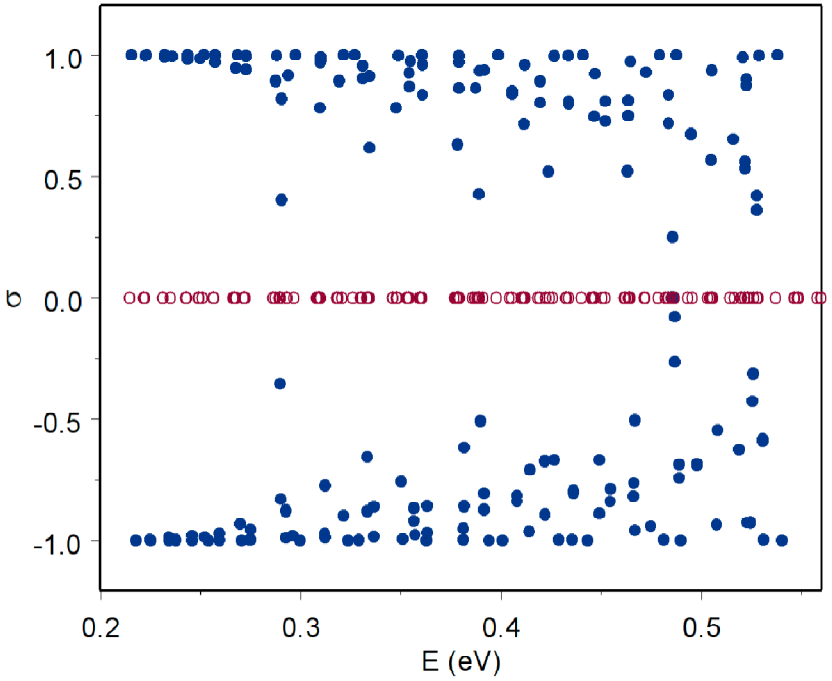

The σ-parameter of the single electron states in InAs/GaAs DQD. Inter-dot distance is a=2 nm. QD radii are 40 nm. Open circles (solid circles) correspond to calculated results without electric filed (with the electric field F =0.25 (kV/cm)).

Strong influence on spectral distribution localized – delocalized states

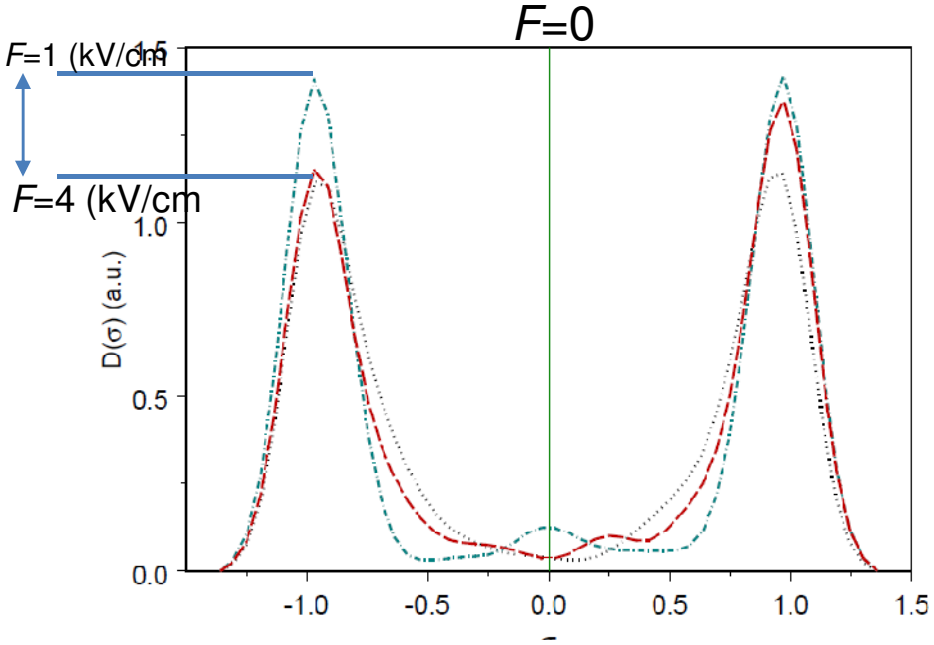

Density functions *D*(sigma) of the sigma-parameter are shown for different values of the electric field. Dot-dashed curve is the result with *F*=1 (kV/cm), dashed curve - with *F*=4 (kV/cm), solid line - with *F*=0, doted curve - *F*=0.25 (kV/cm). Inter-dot distance is a=2 nm; QD radii are 40 nm.

Non-identical lateral IsAs/GaAs QDs in the electric field

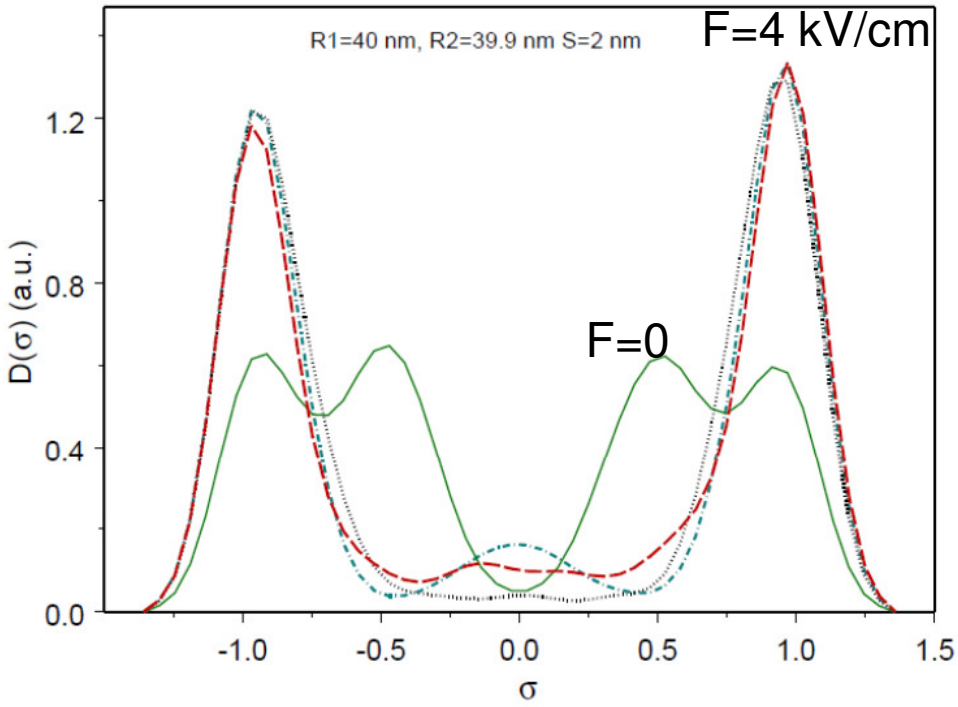

Density functions D(σ) of the σ-parameter for different values of the electric field when ξ=0.9975. (0.25%) Dot-dashed curve corresponds to the result with *F*=1 (kV/cm), dashed curve - with *F*=4 (kV/cm), solid line - with *F*=0, doted curve – with *F*=0.25 (kV/cm).

Inter-dot distance is *a*=2 nm; QD radii are 40 nm.

Relaxation of the delocalization state of DQD

Double concentric quantum ring

Structure of the spectrum DCQR is appeared by σ(E) dependence :

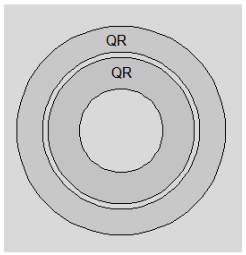

a)

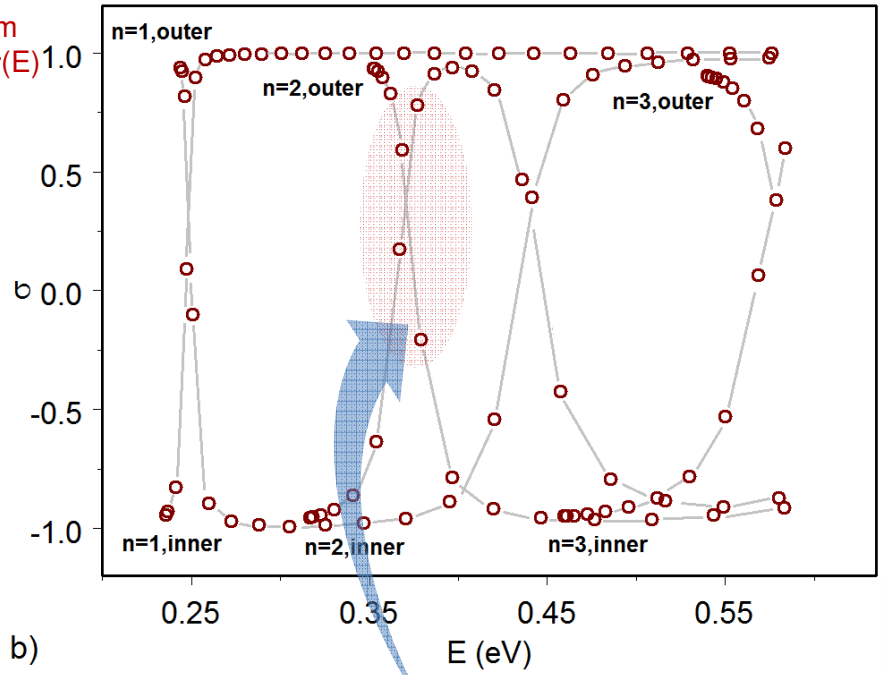

b)

The concentric DQR shape. Geometry parameters are R_1 =30 nm, R_2 =40 nm for outer ring; R_1 =16 nm. R_2 =28 nm for inner ring (the geometry was scaled by factor 1.5). The inter ring distances is 2 nm. b) The σ -parameter for spectrum of concentric DQR. The radial quantum numbers of the each ring are shown in the approximation of "independent rings". The calculated points are connected in order of increasing l =1,2,3.... for each n -band. These traces are created by consequence increasing the orbital quantum number for states with fixed n.

The tunneling between the rings in DCQR is possible for neighboring levels with same symmetry (equal l).

Structure of the spectrum of single QR:

$$E_{n,l} \sim \hbar / 2m^{*}(n^2/W^2 + l^2/R^2)$$

$W << R$ where W is the width of the QR.

Wave functions of delocalized levels:

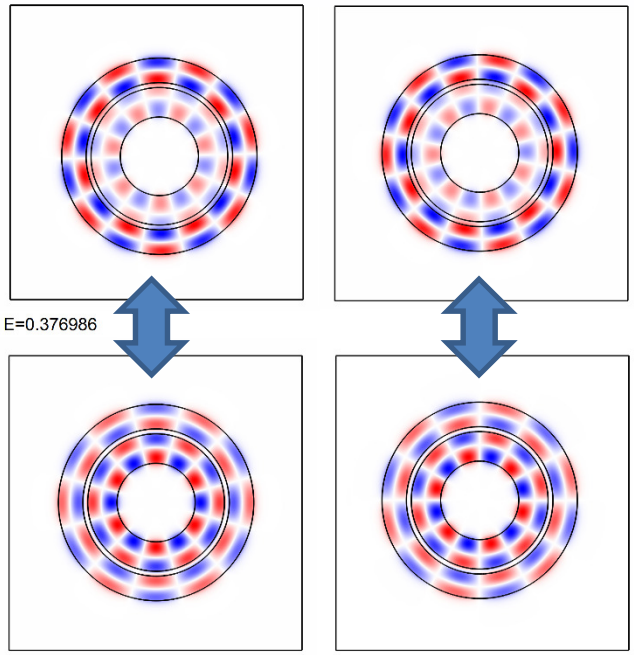

Electron Transition between Weakly Coupled Concentric Quantum Rings and Dots in external magnetic and electric field

Single electron energies and rms of DCQR as a function of magnetic field magnitude

I. Filikhin , S. Matinyan, J. Nimmo, B. Vlahovic, Physica E, **43**, 2011, 1169.

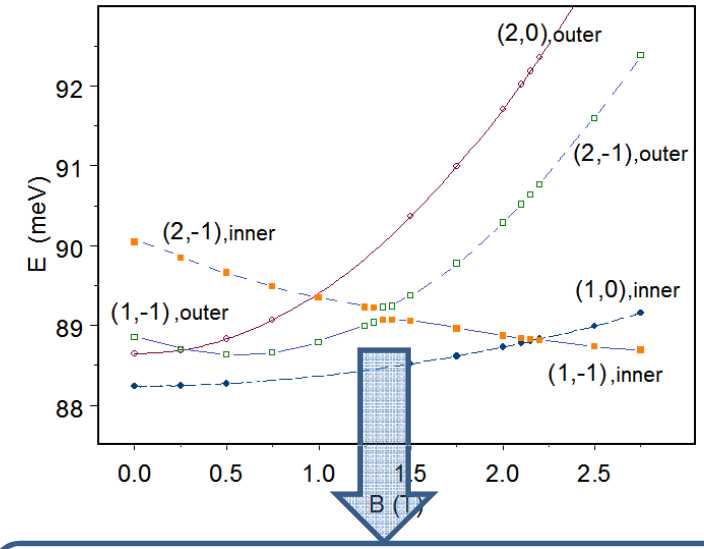

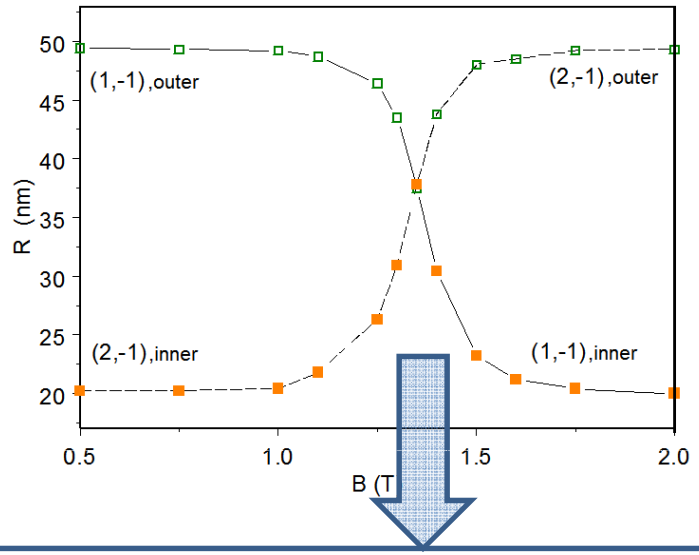

Fabrication

Double concentric quantum rings (DCQR)

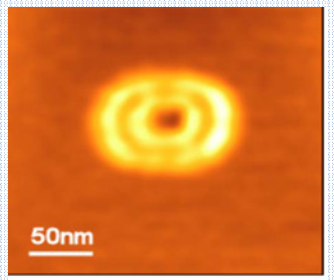

S. Sanguinetti et al,
Phys. Rev. B 77, 125404 (2008)

Anti-crossing levels: *the wave functions have the same type of symmetry (equal orbital quantum numbers)*

Electron transition

Profiles of the normalized square wave function of electron

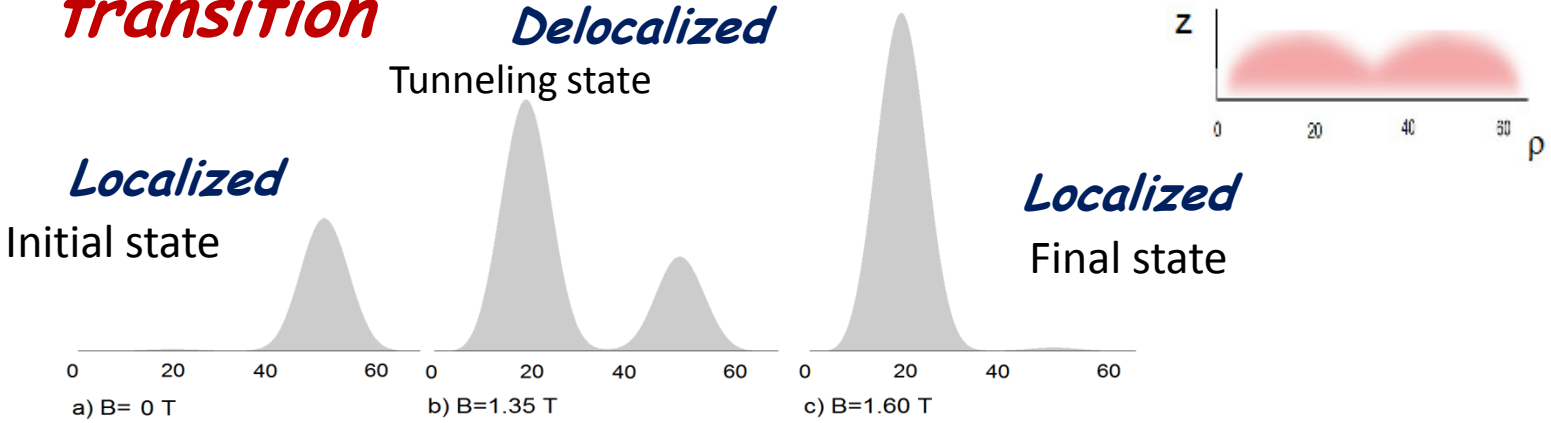

Competition between a) b) and c) gives the effect of the electron transfer between inner and outer rings

Formalism:

- In the single sub-band approach :

$$\left(\hat{H}_{kp} + V_c(\mathbf{r})\right)\Psi(\mathbf{r}) = E\,\Psi(\mathbf{r})$$

For GaAs/$Al_{0.70}Ga_{0.30}As$ QR

$$V_c = \begin{cases} 0 & \text{inside rings} \\ 262\ \text{meV} & \text{inside substrate} \end{cases} \qquad m^* = \begin{cases} 0.067 m_0 & \text{inside rings} \\ 0.093 m_0 & \text{inside substrate} \end{cases}$$

- With the vector potential: $\mathbf{A} = \frac{1}{2} B\rho\hat{\varphi}$, one has in cylindrical coordinates
- $$-\frac{\hbar^2}{2}\left(\frac{1}{\rho}\frac{\partial}{\partial\rho}\left(\frac{\rho}{m^*}\frac{\partial\Psi}{\partial\rho}\right) + \frac{1}{m^*\rho^2}\frac{\partial^2\Psi}{\partial\varphi^2}\right) + \frac{i\hbar qB}{2m^*}\frac{\partial\Psi}{\partial\varphi} + \frac{m^*\left(qB/m^*\right)^2\rho^2}{8}\Psi - \frac{\hbar^2}{2m^*}\frac{\partial^2\Psi}{\partial z^2} + V_c(\rho, z)\Psi = E\,\Psi$$

c) Magnetic field terms

- Solved using FEM utilizing Ben-Daniel-Duke boundary conditions (BDD).

b) term Includes the centrifugal potential

a) term Includes first derivation dividing on ρ

Electron Transitions in Double Quantum Dots due to an Applied Constant External Electric Field

$$-\frac{\hbar^2}{2m^*}\nabla^2\Psi + [V + eF(x - x_0)]\psi = E\psi$$

Anti-crossing of Energy Levels

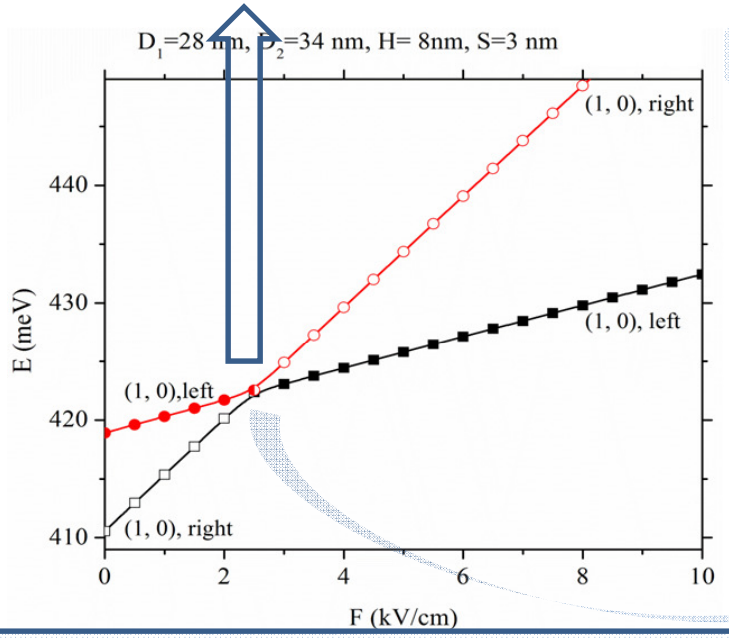

Electron transition between non-identical QDs

Localized

Wave Functions:

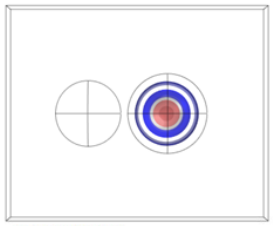

F=2.0 kV/cm;
n=1, l=0, right;
E=420.125 meV

Initial state

F=2.0 kV/cm; n=1, l=0,
transitional;
E=422.349 meV

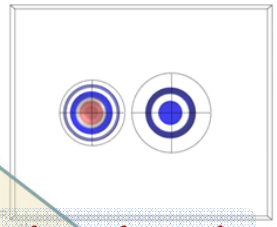

Tunneling states

Delocalized

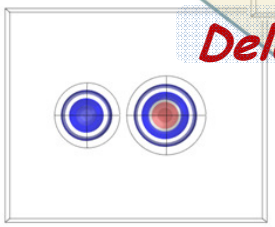

F=2.45 kV/cm; n=1, l=0,
transitional;
E=422.232 meV

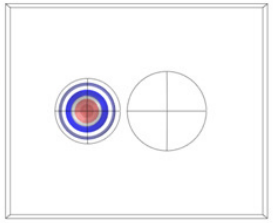

Final state

F=3.0 kV/cm;
n=1, l=0, left;
E=421.691 meV

Localized

Comment

Unlike double concentric quantum rings in the presents of a perpendicular magnetic field, a lateral electric field applied to a DLQD system can cause electrons migrate from one quantum dot to another for ground state, that is easy for experimental preparation.

Conclusions:

1. Inter –ring (inter-dot) electron transition occurs by anti-crossing of levels.
2. Tunneling is the main mechanism for the electron transition.
3. DQD and DCQR may be used in quantum computing

Conclusions

Violation of symmetry of the DQD geometry diminishes the tunneling

High sensitivity of the tunneling on the geometry and external fields change could be of technological interest

Biochemical detector – New principle of operation, highly sensitive and selective

Quantum computing – with external fields it is possible to control tunneling

This work is supported by the NSF (HRD-0833184) and NASA (NNX09AV07A).

Let Us Meet Again

We welcome all to our future group conferences of Omics group international

Please visit:

www.omicsgroup.com

www.Conferenceseries.com

http://optics.conferenceseries.com/